PHYSICAL REVIEW D **93,** 012003 (2016)

Search for vectorlike charge $2/3\,T$ quarks in proton-proton collisions at $\sqrt{(s)} = 8$ TeV

V. Khachatryan *et al.*[*]
(CMS Collaboration)
(Received 14 September 2015; published 19 January 2016)

A search for fermionic top quark partners T of charge 2/3 is presented. The search is carried out in proton-proton collisions corresponding to an integrated luminosity of 19.7 fb^{-1} collected at a center-of-mass energy of $\sqrt{s} = 8$ TeV with the CMS detector at the LHC. The T quarks are assumed to be produced strongly in pairs and can decay into tH, tZ, and bW. The search is performed in five exclusive channels: a single-lepton channel, a multilepton channel, two all-hadronic channels optimized either for the bW or the tH decay, and one channel in which the Higgs boson decays into two photons. The results are found to be compatible with the standard model expectations in all the investigated final states. A statistical combination of these results is performed and lower limits on the T quark mass are set. Depending on the branching fractions, lower mass limits between 720 and 920 GeV at 95% confidence level are found. These are among the strongest limits on vectorlike T quarks obtained to date.

DOI: 10.1103/PhysRevD.93.012003

I. INTRODUCTION

The discovery of a Higgs boson with a mass of 125 GeV by the ATLAS [1] and CMS [2,3] collaborations motivates the search for exotic states involving the newly discovered particle. The nature of electroweak symmetry breaking and the mechanism that stabilizes the mass of the Higgs particle are not entirely clear. These questions could be explained by physics beyond the standard model (SM), such as supersymmetry. Nonsupersymmetric explanations are given by little Higgs models [4,5], models with extra dimensions [6,7], and composite Higgs models [6–8] in which the Higgs boson appears as a pseudo-Nambu-Goldstone boson [9]. These theories predict the existence of heavy vectorlike quarks. The left-handed and right-handed components of vectorlike quarks transform in the same way under the electroweak symmetry group, in contrast to the SM fermions, which transform as chiral particles under the SM symmetry group $\mathrm{SU}(3)_c \times \mathrm{SU}(2)_L \times \mathrm{U}(1)_Y$. This property of the vectorlike quarks allows direct mass terms in the Lagrangian of the form $m\bar{\psi}\psi$ that do not violate gauge invariance. As a consequence, and in contrast to the other quark families, vectorlike quarks do not acquire their mass via Yukawa couplings. In many of the models mentioned above the vectorlike quarks couple predominantly to the third generation quarks only. This means that they may have the following three decay modes: tH, tZ, and bW [10]. A model of vectorlike T quarks with charge $2/3e$, which are produced in pairs via strong interaction, is used as a benchmark for this analysis.

A fourth generation of chiral fermions, replicating one of the three generations of the SM with identical quantum numbers, is disfavored by electroweak fits within the framework of the SM [11]. This is mostly because of large modifications of the Higgs production cross sections and branching fractions ($\mathcal{B}$), if a single SM-like Higgs doublet is assumed. Heavy vectorlike quarks decouple from low energy loop-level electroweak corrections and are not similarly constrained by the measurements of the Higgs boson properties [10].

Early T quark searches by the CMS Collaboration [12–14] have assumed 100% branching fractions to various final states. More recent searches [15] do not make specific assumptions for the branching fractions. Searches for T quarks have been performed also by the ATLAS Collaboration, setting lower limits on the T quark mass ranging from 715 to 950 GeV, for different T quark branching fractions [16–18].

In this paper, results of searches for T quark production in proton-proton collisions, using the CMS detector at the CERN LHC, are presented for five different decay modes. One of the searches [15] is inclusive and sets limits for all possible branching fractions. This analysis is based on leptonic final states and is described in Sec. V A. The other four analyses have a good sensitivity in optimized regions, but they do not cover the full range of branching fractions. The analysis described in Sec. V B is specifically optimized to find $T \to bW$ decays. The searches presented in Sec. V C and Sec. V D are optimized for all-hadronic final states in

[*]Full author list given at the end of the article.

the decays $T \to bW$ and $T \to tH$. The search discussed in Sec. V E is sensitive to $T \to tH$ decays, where the Higgs boson decays to a pair of photons. The two analyses presented in Secs. V A and V C are discussed in detail in separate publications [15,19]. The remaining three analysis are published here for the first time.

The CMS detector is briefly described in Sec. II. Section III describes the data and the simulated samples. Section IV gives details about the reconstruction techniques used by the analyses. Section VI describes the combination and the treatment of systematic uncertainties. Section VII presents the results of the combination.

II. THE CMS DETECTOR

The central feature of the CMS apparatus is a superconducting solenoid of 6 m internal diameter, providing a magnetic field of 3.8 T. Within the solenoid volume are a silicon pixel and strip tracker, a lead tungstate crystal electromagnetic calorimeter (ECAL), and a brass and scintillator hadron calorimeter (HCAL), each composed of a barrel and two endcap sections. Muons are measured in gas-ionization detectors embedded in the steel flux-return yoke outside the solenoid. Extensive forward calorimetry complements the coverage provided by the barrel and endcap detectors.

In the region of pseudorapidity $|\eta| < 1.74$ [20], the HCAL cells have widths of 0.087 in η and 0.087 radians in azimuth (ϕ). In the η-ϕ plane, and for $|\eta| < 1.48$, the HCAL cells map on to 5×5 ECAL crystals arrays to form calorimeter towers projecting radially outwards from close to the nominal interaction point. At larger values of $|\eta|$, the size of the towers increases and the matching ECAL arrays contain fewer crystals. Within each tower, the energy deposits in ECAL and HCAL cells are summed to define the calorimeter tower energies, subsequently used to provide the energies and directions of hadronic jets.

The electron momentum is estimated by combining the energy measurement in the ECAL with the momentum measurement in the tracker. The momentum resolution for electrons with transverse momentum $p_T \approx 45$ GeV from $Z \to ee$ decays ranges from 1.7% for nonshowering electrons in the barrel region to 4.5% for showering electrons in the endcaps [21]. The energy resolution for photons with transverse energy $E_T \approx 60$ GeV varies between 1.1% and 2.6% in the ECAL barrel, and from 2.2% to 5% in the endcaps [22].

The silicon tracker measures charged particles within the pseudorapidity range $|\eta| < 2.5$. It consists of 1440 silicon pixel and 15 148 silicon strip detector modules. For nonisolated particles of $1 < p_T < 10$ GeV and $|\eta| < 1.4$, the track resolutions are typically 1.5% in p_T and 25–90 (45–150) μm in the transverse (longitudinal) impact parameter [23].

A more detailed description of the CMS detector, together with a definition of the coordinate system used and the relevant kinematic variables, can be found in Ref. [20].

III. EVENT SAMPLES

This analysis makes use of data recorded with the CMS detector in proton-proton collisions at a center-of-mass energy of $\sqrt{s} = 8$ TeV corresponding to an integrated luminosity of 19.5 fb^{-1} for the analysis described in Sec. V A, and 19.7 fb^{-1} for the other analyses.

Events are selected by a multistage trigger system. The single-lepton channels are based on single-muon and single-electron triggers. The single-muon sample is obtained by the requirement of an isolated muon candidate, with high-level trigger thresholds of $p_T > 24$ GeV (inclusive search, Sec. V A) or $p_T > 40$ GeV (single-lepton search, Sec. V B). In the electron sample, a single isolated electron trigger with $p_T > 27$ GeV is required. Multilepton events are selected by requiring at least two lepton candidates, one with $p_T > 17$ GeV and the other with $p_T > 8$ GeV in the high-level trigger. The all-hadronic final states require large hadronic activity in the detector, namely that the scalar p_T sum of reconstructed jets is larger than 750 GeV. This quantity is evaluated in the high-level trigger from jets with $p_T > 40$ GeV using calorimeter information only. For searches in the diphoton final state, two photons are required. The photon E_T thresholds in the high-level trigger are 26 (18) GeV and 36 (22) GeV on the leading (subleading) photon, depending on the running period.

The contributions from SM processes are generally predicted using simulated event samples. For some backgrounds, however, the simulations are not fully reliable, and control samples of data are used to determine their contribution. The background estimation for the individual channels is discussed in Sec. V.

Standard Model background events are simulated using POWHEG v1.0 [24–26] for $t\bar{t}$ and single t production; MADGRAPH 5.1 [27] for W + jets, Z + jets, $t\bar{t}W$, and $t\bar{t}Z$ production; and PYTHIA 6.426 [28] for WW, WZ, ZZ, and $t\bar{t}H$ processes.

For W + jets and Z + jets production, samples with up to four partons are generated and merged using the MLM scheme with k_T jets [29,30]. The CTEQ6M parton distribution functions (PDF) are used for POWHEG, while for the other generators the CTEQ6L1 [31] PDFs are used. In all cases, PYTHIA 6.426 [28] is used to simulate the hadronization and the parton showering.

The $T\bar{T}$ signal process is simulated using MADGRAPH 5.1, allowing up to two additional hard partons. A series of mass hypotheses between 500 and 1000 GeV are generated in steps of 100 GeV. The inclusive cross sections for the signal samples and the $t\bar{t}$ samples are calculated at next-to-next-to-leading order (NNLO) for $gg \to t\bar{t} + X$. The fixed-order calculations are supplemented with soft-gluon resummations having next-to-next-to-leading logarithmic accuracy [32]. The $t\bar{t}$ cross sections are

TABLE I. The NNLO $T\bar{T}$ pair production cross section for different values of the T quark mass.

T quark mass (GeV)	Production cross section (pb)
500	0.59
600	0.17
700	0.059
800	0.021
900	0.0083
1000	0.0034

computed based on the TOP++ v2.0 implementation using the MSTW2008nnlo68cl PDFs and the 5.9.0 version of LHAPDF [32,33]. The $t\bar{t}$ cross section is computed to be 252.9 pb, assuming a top quark mass of 172.5 GeV. The model-independent cross sections calculated for the signal samples are listed in Table I.

Minimum bias interactions are generated using PYTHIA and are superimposed on the simulated events to mimic the effect of additional proton-proton collisions within a single bunch crossing (pileup). The pileup distributions of the simulated signal and background events match that observed in data, with an average of 21 reconstructed collisions per beam crossing.

IV. EVENT RECONSTRUCTION

Tracks are reconstructed using an iterative tracking procedure [23]. The primary vertices are reconstructed with a deterministic annealing method [34] from all tracks in the event that are compatible with the location of the proton-proton interaction region. The vertex with the highest $\sum(p_{\mathrm{T}}^{\mathrm{track}})^2$ is defined as the primary interaction vertex (PV), whose position is determined from an adaptive vertex fit [35].

The particle-flow event reconstruction algorithm [36,37] reconstructs and identifies each individual particle, using an optimized combination of information from the various elements of the CMS detector. The energy of muons is obtained from the curvature of the corresponding track. The energy of electrons is determined from a combination of the electron momentum at the PV as determined by the tracker, the energy of the corresponding ECAL cluster, and the energy sum of all bremsstrahlung photons spatially compatible with originating from the electron track. The energy of charged hadrons is determined from a combination of their momentum measured in the tracker and the matching ECAL and HCAL energy deposits, corrected for zero suppression effects and for the response function of the calorimeters to hadronic showers. Finally, the energy of neutral hadrons is obtained from the corresponding corrected ECAL and HCAL energies.

Muon (electron) candidates are required to originate from the PV and to be isolated within $\Delta R = \sqrt{(\Delta\eta)^2 + (\Delta\phi)^2} < 0.4(0.3)$ around the lepton direction, where $\Delta\eta$ ($\Delta\phi$) indicates the difference in pseudorapidity η (ϕ) from the lepton direction. The degree of isolation is quantified by the ratio of the p_{T} sum of all additional particles reconstructed in the isolation cone to the p_{T} of the lepton candidate. This ratio for a muon (electron) is required to be less than 0.12 (0.10). Together with the lepton identification requirements, the isolation conditions strongly suppress backgrounds from jets containing leptons.

Photons are identified as ECAL energy clusters not linked to the extrapolation of any charged particle trajectory to the ECAL. The energy of photons is directly obtained from the ECAL measurement, corrected for zero-suppression effects. In the ECAL barrel section, an energy resolution of about 1% is achieved for unconverted or late-converting photons in the tens of GeV energy range. The remaining barrel photons are measured with an energy resolution of about 1.3% up to $|\eta| = 1$, rising to about 2.5% at $|\eta| = 1.4$. In the endcaps, the resolution of unconverted or late-converting photons is about 2.5%, while all other photons have a resolution between 3 and 4% [38].

For each event, hadronic jets are reconstructed by applying the anti-k_{T} (AK) algorithm [39,40] and/or the Cambridge–Aachen (CA) [41] jet clustering algorithms to the reconstructed particles. The AK algorithm is used with a jet size parameter of 0.5 (AK5 jets). In some analyses both algorithms are used. The algorithms are applied independently of each other to the full set of reconstructed particles. Charged particles that do not originate from the PV are removed from the jets. The momentum of each jet is defined as the vector sum of all particle momenta in the jet cluster, and is found in the simulation to be within 5% to 10% of the true particle-level momentum over the whole p_{T} spectrum and detector acceptance. Jet energy corrections are derived from the simulation, and are confirmed with measurements of the energy balance of dijet and photon + jet events [42]. The jet energy resolution is typically 15% at 10 GeV, 8% at 100 GeV, and 4% at 1 TeV, to be compared to about 40%, 12%, and 5% obtained when the calorimeters alone are used for jet clustering.

Neutrinos escape the detector undetected and give rise to the missing transverse momentum vector, defined as the projection on the plane perpendicular to the beams of the negative vector sum of the momenta of all reconstructed particles in an event. Its magnitude is referred to as $E_{\mathrm{T}}^{\mathrm{miss}}$.

The jets contain neutral particles from pileup events. The contribution from these additional particles is subtracted based on the average expectation of the energy deposited from pileup in the jet area, using the methods described in Ref. [43].

For the identification of jets resulting from fragmentation of b quarks (“b jets”), an algorithm is used that combines information from reconstructed tracks and from secondary vertices, both characterized by a displacement with respect to the PV. This information is combined into a single discriminating variable and jets are tagged as b jets based on its value. The algorithm is referred to as "combined secondary vertex tagger" and is described in Ref. [44]. In most of the analyses described in the following, a minimum value of this variable (medium operating point) is chosen such that the b tagging efficiency is 70% and the light-flavor jet misidentification rate is 1% in $t\bar{t}$ events. The analyses presented in Secs. V B and V E also use a smaller minimum value of the discriminating variable (loose operating point), yielding a higher efficiency of approximately 80%, with a light-flavor misidentification rate of 10%.

A. Jet substructure methods

Because of the possible large mass of the T quarks, the top quarks, Higgs and W bosons from T quark decays might have significant Lorentz boosts. Daughter particles produced in these decays would therefore not be well separated. In many cases, all decay products are clustered into a single large jet by the event reconstruction algorithms. These merged jets exhibit an intrinsic substructure that can be analyzed with dedicated jet substructure algorithms. In order to cluster the decay products from top quarks and Higgs boson into wide jets, the CA algorithm is used with size parameters $\mathrm{R} = 1.5$ (CA15 jets) or $\mathrm{R} = 0.8$ (CA8 jets). A number of jet substructure algorithms are then used in different analyses to identify jets from top quark or Higgs boson decays. This process is known as t or H tagging, and in some cases relies on b tagging of individual subjets.

The inclusive T quark search in final states with leptons discussed in Sec. V A uses the CMSTOPTAGGER [45], which is based on the algorithm developed in Ref. [46]. The tagger identifies a top quark decay if a CA8 jet with $p_{\mathrm{T}} > 400$ GeV is found with a mass between 140 and 250 GeV and at least three subjets with a minimum mass of subjet pairs larger than 50 GeV. The sensitivity of the CMSTOPTAGGER is suitable for a regime with jet $p_{\mathrm{T}} > 400$ GeV where the decay products are collimated to be within the acceptance of a jet with the size parameter of 0.8.

The search for $T \to tH$ in the hadronic final state (Sec. V C) adopts the HEPTOPTAGGER algorithm [47,48], which employs CA15 jets to increase the acceptance to top quarks with a moderate Lorentz boost ($p_{\mathrm{T}} > 200$ GeV). This facilitates a smooth transition between the boosted and resolved regimes. A CA15 t jet candidate is required to exhibit a substructure compatible with a three-body decay. If this requirement is satisfied, the HEPTOPTAGGER clustering algorithm identifies the three subjets, and then requires that the mass of a subjet pair be consistent with the W boson mass and the mass of the three subjets be consistent with the top mass. The t tagging performance is further enhanced by the application of b tagging to subjets of CA15 jets [49]. Subjet b tagging is also used to identify decays of boosted Higgs bosons into a bottom quark-antiquark pair. The subjets of CA15 jets are reconstructed using the filtering algorithm described in Ref. [50]. Two filtered subjets of CA15 jets are required to have a di-subjet invariant mass larger than 60 GeV. Both subjets are tagged using the subjet b tagging algorithm, which is based on the same algorithm used for regular anti-k_{T} jets, discussed above, with the difference that only tracks and secondary vertices associated with the individual subjets are used to build the b tag discriminator.

For the identification of boosted W bosons, two subjets are required to be reconstructed by a pruning algorithm [50–52]. The mass of the pruned jet has to be compatible with the mass of the W boson, within a mass window that differs slightly depending on the analysis considered. The inclusive analysis in Sec. V A requires a W jet to have $p_{\mathrm{T}} > 200$ GeV and a mass between 60 and 130 GeV. The search for $T \to bW$ with single leptons (Sec. V B) applies the same p_{T} selection, but the mass window is tightened to 60 to 100 GeV. The search for $T \to bW$ in hadronic final states (Sec. V D) requires $p_{\mathrm{T}} > 150$ GeV in combination with a jet mass m_{j} requirement of $60 < m_{\mathrm{j}} < 100$ GeV. Additionally, this analysis complements pruning with a selection on the mass drop [50], which is defined as the ratio of the largest subjet mass to that of the original jet. Requiring the mass drop to be < 0.4 rejects events containing massive jets from QCD multijet processes.

The different performance of the t tagging and W tagging algorithms in data and simulation is taken into account with scale factors that are applied to the simulated events [48,53].

V. ANALYSIS CHANNELS

In this section, five distinct searches for T quarks are presented, each optimized for a different topology. The analyses described in Secs. V A and V B are based on leptonic final states. While the former is an inclusive search covering all possible decay modes, the latter is a search specifically optimized to find $T \to bW$ decays. The searches presented in Sec. V C and Sec. V D are optimized for boosted event topologies in hadronic final states and make use of jet substructure techniques. Finally, the search treated in Sec. V E is sensitive to $T \to tH$ decays, where the Higgs boson decays to a pair of photons.

A. Inclusive search with single and multiple leptons

The inclusive search described in this section is sensitive to all decay modes of the T quark, i.e., $T \to tH$, $T \to tZ$, and $T \to bW$. It is divided into two channels: one channel in which exactly one lepton is selected and the other channel with at least two leptons. Further details are given in Ref. [15].

1. Single-lepton channel

Single-lepton events must contain exactly one isolated muon or electron with $p_{\mathrm{T}} > 32$ GeV. In addition to the lepton, events must also have at least three AK5 jets with $p_{\mathrm{T}} > 120$, 90, and 50 GeV. A fourth AK5 jet with $p_{\mathrm{T}} > 35$ GeV is required if no W jet is identified in the

TABLE II. Main selection requirements for the single-lepton analysis.

Variable	Selection
p_{T} lepton	>32 GeV
Number of jets	≥3
p_{T} jets	>120, 90, and 50 GeV
W tag	≥1 or ≥1 jets with $p_{\mathrm{T}} > 35$ GeV
$E_{\mathrm{T}}^{\mathrm{miss}}$	>20 GeV

event. To fulfill the lepton isolation requirement, jets must be separated by $\Delta R > 0.4$ from muons and by $\Delta R > 0.3$ from electrons. The requirement on the jet multiplicity and p_{T} significantly suppresses background processes. The contribution from QCD multijet events is further reduced by selecting events with $E_{\mathrm{T}}^{\mathrm{miss}} > 20$ GeV. The major selection requirements are summarized in Table II.

Some background events from $W+$jets production remain after the event selection. This process is not well modeled by simulations and the normalization is determined from a control sample in data. This sample is defined by single-lepton events fulfilling the signal selection criteria, but failing the requirement that a fourth jet with $p_{\mathrm{T}} > 35$ GeV or alternatively a W jet is identified in the event.

A boosted decision tree (BDT) [54] is used to discriminate between signal and background events. Different BDTs are implemented for events with and without identified W jets and for each hypothetical value of the mass of the T quark. The use of dedicated BDTs for different T quark decay modes does not improve the performance, so the BDTs are trained irrespective of the branching fraction of the T quark.

The variables used for the calculation of the BDT discriminant are jet multiplicity, b -tagged jet multiplicity, $E_{\mathrm{T}}^{\mathrm{miss}}$, lepton p_{T}, p_{T} of the third jet, p_{T} of the fourth jet, and H_{T}, where H_{T} is defined as the scalar p_{T} sum of all jets with $p_{\mathrm{T}} > 30$ GeV. For events with at least one W jet, the multiplicity and p_{T} of W-tagged jets and the numbers of t-tagged jets are also included in the BDT training. These variables are chosen based on their discrimination power as calculated by the BDT algorithm, and on the absence of significant correlations between the different variables. The final BDT distributions are shown in Ref. [15]. The total numbers of events predicted for background processes and observed in collision data are shown in Table III.

TABLE III. Numbers of events predicted for background processes and observed in collision data for the single-lepton analysis. The uncertainties include those in the luminosity, the cross sections and the correction factors on lepton and trigger efficiencies. From Ref. [15].

	Muon	Electron
Total background	61900 ± 13900	61500 ± 13700
Data	58478	57743

The predicted contributions for each background process are available in Ref. [15]. The signal selection efficiencies are between 7.5% and 9.4% which corresponds to an expected number of 850 events for a T quark mass of 500 GeV and 6 events for a T quark mass of 1000 GeV assuming branching fractions to tH, tZ, and bW of 25%, 25%, and 50%, respectively. A detailed table with selection efficiencies and expected number of events is available in Ref. [15].

2. Multilepton channel

This channel uses four mutually exclusive subsamples with at least two leptons: two opposite-sign dilepton samples (referred to as *OS*1 and *OS*2 samples) which differ by the required numbers of jets in the event, a same-sign dilepton sample (the *SS* sample) and a multilepton sample. The division into opposite- and same-sign dilepton events is based on the charge of the leptons.

Multilepton events must contain at least three leptons with $p_{\mathrm{T}} > 20$ GeV. To reject backgrounds from heavy-flavor resonances and low-mass Drell–Yan (DY) production, multilepton events must contain a dilepton pair of the same flavor and of opposite charge with an invariant mass above 20 GeV. Events in which $E_{\mathrm{T}}^{\mathrm{miss}} \leq 30$ GeV are discarded. Jets must be separated by $\Delta R > 0.3$ from the selected leptons and at least one of the jets has to fulfill the b tagging criteria.

The *OS*1 dilepton sample targets events in which both T quarks decay to bW [13]. This dilepton sample contains events with either two or three jets, $H_{\mathrm{T}} > 300$ GeV, and $S_{\mathrm{T}} > 900$ GeV, where S_{T} is the sum of H_{T}, $E_{\mathrm{T}}^{\mathrm{miss}}$, and the transverse momenta of all leptons. Events are discarded where there is a dilepton pair with same-flavor leptons and a mass $M_{\ell\ell}$ consistent with that of a Z boson ($76 < M_{\ell\ell} < 106$ GeV). To reduce the $t\bar{t}$ background, all the possible pair-wise combinations of a lepton and a b jet are considered and their invariant masses are all required to be larger than 170 GeV.

The DY background is not modeled reliably in the selected kinematic region and is controlled using a data sample consisting of events with no b-tagged jets, $E_{\mathrm{T}}^{\mathrm{miss}} < 10$ GeV, $S_{\mathrm{T}} < 700$ GeV, and $H_{\mathrm{T}} > 300$ GeV.

The *OS*2 dilepton sample consists of events with at least five jets, two of which must be identified as b jets. Events are also required to have $H_{\mathrm{T}} > 500$ GeV, and $S_{\mathrm{T}} > 1000$ GeV. This sample is mostly sensitive to signal events where both T quarks decay to tZ. The dominant background is $t\bar{t}$ production.

The *SS* sample selection criteria target events in which at least one T quark decays to tZ or tH. Besides the lepton selection criteria, at least three jets are required, $H_{\mathrm{T}} > 500$ GeV, and $S_{\mathrm{T}} > 700$ GeV.

Different processes contribute to the background in the *SS* sample. A minor contribution is given by SM processes leading to prompt *SS* dilepton signatures, which have very small cross sections. These processes can be simulated reliably. The prompt OS dilepton production can also contribute if one lepton is misreconstructed with the wrong sign of the charge. The misreconstruction probability of the charge sign is negligible for muons in the kinematic range considered, while for electrons it is determined from control data samples. We determine the probability to misreconstruct the charge sign of an electron from events with a dileptonic Z decay, selected with the same criteria as in the signal selection except for the charge requirement. Instrumental backgrounds in which misidentified jets create lepton candidates are determined from control data samples in which nonprompt and fake leptons are enriched.

The multilepton sample, like the SS sample, is mostly sensitive to signal events in which at least one T quark decays to tZ or tH. The backgrounds are suppressed by selecting events with at least three jets, $H_{\mathrm{T}} > 500$ GeV, and $S_{\mathrm{T}} > 700$ GeV. Prompt backgrounds in this channel are due to SM processes with three or more leptons in the final state, such as diboson and triboson production. These are correctly modeled by simulation. Nonprompt backgrounds are caused by the misidentification of one or more leptons, by $t\bar{t}$ production, and by other processes. As for the dilepton samples, data control samples are used to evaluate these sources of background.

The main selection requirements for the four samples are summarized in Table IV.

The numbers of events in the multilepton samples are given in Table V, both for data and for estimated background contributions. The predicted contributions for each background process are available in Ref. [15]. The selection efficiencies for signal events are between 0.15% and 0.44% which corresponds to an expected number of 16.7 events for a T quark mass of 500 GeV and 0.28 events for a T quark mass of 1000 GeV, assuming branching fractions to tH, tZ, and bW of 25%, 25%, and 50%, respectively. A detailed table with selection efficiencies and expected number of events is available in Ref. [15]. The numbers of background and signal events are of similar order of magnitude. The sensitivity to the signal is enhanced by further splitting the samples according to the lepton flavor. The dilepton samples are separated into three subsamples, $\mu\mu$, μe, and ee. The multilepton sample is divided into a $\mu\mu\mu$ subsample, an eee subsample, and a third subsample with events with mixed lepton flavors. Data and SM background expectations are found to be in agreement.

TABLE IV. Main selection requirements for the four multilepton channels: the opposite-sign dilepton samples with two or three jets ($OS1$) and with at least five jets ($OS2$), the same-sign dilepton sample (SS), and the multilepton sample. The smallest mass obtained from all the possible combinations of leptons and b jets is indicated by $M_{b\ell}$.

	$OS1$	$OS2$	SS	Multileptons
H_{T} (GeV)	>300	>500	> 500	>500
S_{T} (GeV)	>900	>1000	>700	>700
Number of jets	2 or 3	≥5	≥3	≥3
b tags	≥1	≥ 2	≥1	≥1
$E_{\mathrm{T}}^{\mathrm{miss}}$ (GeV)	>30	> 30	>30	>30
$M_{b\ell}$ (GeV)	>170	...	...	...
$M_{\ell\ell}$ (GeV)	>20	>20	>20	>20
Z boson veto	Yes	No	No	No

TABLE V. Numbers of events selected in data and expected for the backgrounds. Shown are the opposite-sign dilepton samples with two or three jets ($OS1$) and with at least 5 jets ($OS2$), the same-sign dilepton sample (SS), and the multilepton sample. The background sources not contributing to the channel are indicated by a dash ("–"). The uncertainties include statistical, normalization, and luminosity uncertainties. From Ref. [15].

	$OS1$	$OS2$	SS	Multileptons
Total background	17.4 ± 3.7	84 ± 12	16.5 ± 4.8	3.7 ± 1.3
Data	20	86	18	2

B. Search for $T \to bW$ with single leptons

The analysis described in this section is optimized for the event topology in which both T quarks decay into a bottom quark and a W boson.

Events are required to have one isolated muon or electron, where muon candidates must have $p_{\mathrm{T}} > 45$ GeV and electron candidates must have $p_{\mathrm{T}} > 30$ GeV. At least four jets are required, either at least four AK5 jets or at least three AK5 jets plus at least one CA8 jet. The AK5 jets are required to have $p_{\mathrm{T}} > 30$ GeV and CA8 jets are required to have $p_{\mathrm{T}} > 200$ GeV. Both types of jets must have $|\eta| < 2.4$.

The CA8 jets are used to identify merged hadronic decays of W bosons with high Lorentz boost. The AK5 jets are replaced by the two pruned subjets of W-tagged CA8 jets if the angular distance between AK5 and CA8 jets fulfills the matching criterion $\Delta R(\mathrm{Jet}_{\mathrm{CA8}}, \mathrm{Jet}_{\mathrm{AK5}}) < 0.04$. Unmatched AK5 jets and the subjets of matched W-tagged CA8 jets are used as input for a kinematic fit, which is described below. The four jets or subjets are required to satisfy $p_{\mathrm{T}} > 120$, 90, 50, and 30 GeV. At least one of the AK5 jets has to satisfy the b tagging criteria.

A kinematic fit is made to each event for the hypothesis $T\bar{T} \to bW^{+}\bar{b}W^{-} \to \ell\nu bq\bar{q}'\bar{b}$, subject to the constraints, $m(\ell\nu) = m(q\bar{q}') = M_W$, and $m(\ell\nu b) = m(q\bar{q}'b) = M_{\mathrm{fit}}$, the fitted mass of the selected T candidate. The $E_{\mathrm{T}}^{\mathrm{miss}}$ in the event is attributed to the undetected neutrino from leptonic W decays. If a selected event has more than four jets, the fifth jet with highest p_{T} is also considered and all the possible combinations of four jets are tested in the kinematic fit.

Only events containing fit combinations with χ^2 probability $p(\chi^2) > 1\%$ are retained. The efficiency of the $p(\chi^2)$ criterion is 62% for signal events with a T quark mass of 800 GeV while 76% of background events are rejected. The $p(\chi^2)$ criterion removes badly reconstructed

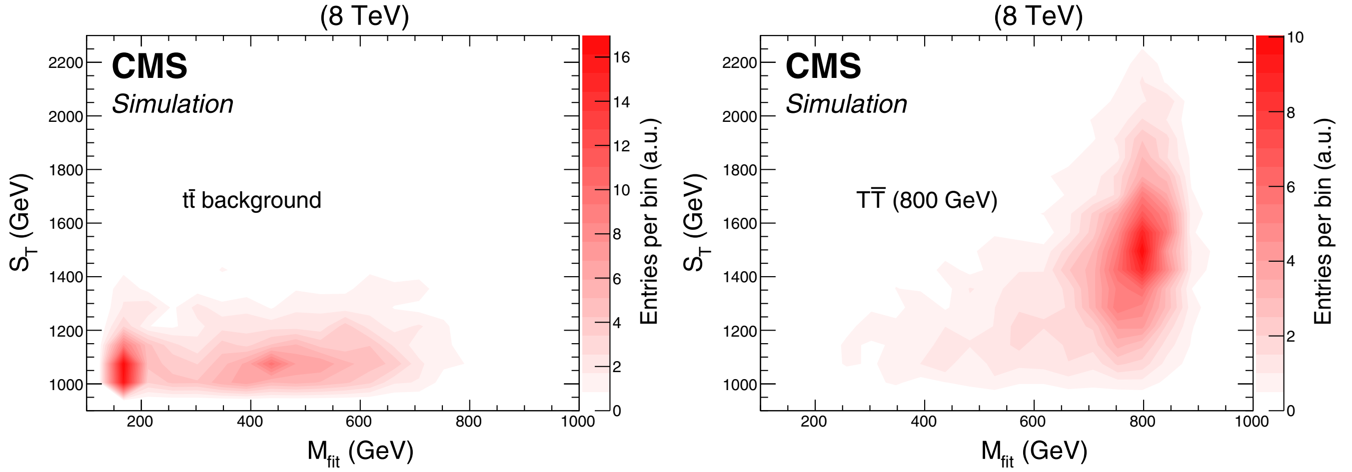

FIG. 1. Correlation between the S_T and the M_{fit} observables in the search for $T \to bW$ with single leptons, for background processes (left) and for a simulated signal, with a T quark mass of 800 GeV (right). The color gradient indicates the entries per bin in arbitrary units (a.u.).

events with poor mass resolution and improves the signal-to-background ratio in the reconstructed mass spectrum.

To reduce the large combinatorial background, the b tagging and the W tagging information is used. If a W tag is present, only those combinations where the subjets of the W jet match the W decay products are considered. The best combination is selected from groups of fit combinations with decreasing b tag multiplicity, ranked by the b tagging operating point (OP), as listed below:

(i) 2 b tags at medium OP;
(ii) 1 b tag at medium OP and 1 b tag at loose OP;
(iii) 1 b tag at medium OP;
(iv) 2 b tags at loose OP.

Decay products of T quarks have on average higher p_T than those from the SM backgrounds. To suppress the backgrounds and enhance the signal significance, we select events with large values of the S_T variable, which is defined here as a sum of E_T^{miss}, p_T of the lepton, and p_T of the four jets that minimize the χ^2 in the kinematic fit. Figure 1 demonstrates that SM backgrounds and a T quark signal populate different regions in the two-dimensional S_T and M_{fit} distribution.

We test the modeling of the shape of the reconstructed mass, and verify how well the SM background expectations agree with data, as a function of S_T. Figure 2 shows the reconstructed mass distributions separately for $\mu +$jets and $e +$jets events with the $S_T > 1000$ GeV requirement.

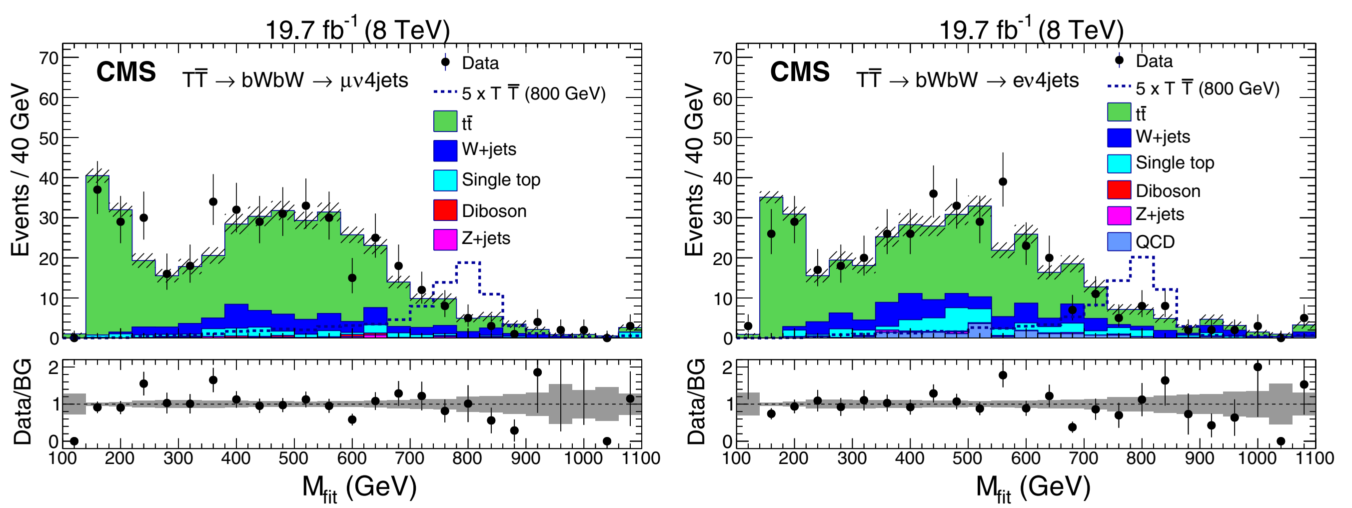

FIG. 2. Distributions of the reconstructed mass M_{fit} for $\mu +$jets (left) and $e +$jets (right) events. The data are shown as points and the simulated backgrounds as shaded histograms. The hatched region and the shaded area in the lower panel represent the statistical uncertainty in the background. The expected signal (dotted line) for a T quark with a mass of 800 GeV is multiplied by a factor of 5 for better visibility. The lower panel represents the ratio between data and the sum of the backgrounds (BG). The overflow of the distributions is added to the last bin.

TABLE VI. Numbers of observed and expected background events after the event selection. The uncertainties in the predicted numbers of events include both the statistical and systematic uncertainties.

	Selection ($S_T > 1000$ GeV)		Selection ($S_T > 1240$ GeV)	
	μ + jets	e + jets	μ + jets	e + jets
$t\bar{t}$	325 ± 37	279 ± 35	51 ± 6	52 ± 6
$W+\geq 3$ jets	49 ± 8	60 ± 9	18 ± 3	19 ± 4
Single top	20 ± 5	36 ± 10	6.9 ± 2.3	10 ± 4
$Z/\gamma^* + \geq 3$ jets	3.9 ± 0.8	3.3 ± 0.6	1.4 ± 0.4	1.1 ± 0.3
WW, WZ, ZZ	3.1 ± 1.0	<1	<1	<1
Multijet	<1	18 ± 4	<1	6.1 ± 1.7
Total background	401 ± 38	396 ± 38	77 ± 7	88 ± 9
Data	417	398	81	83

Correctly reconstructed $t\bar{t}$ events peak near the top quark mass value, while events with misassigned jets constitute a combinatorial background, and populate a region of higher masses, where the potential signal is expected to appear. Table VI (left columns) presents the event yields of SM backgrounds and data for this selection. The dominant background process is $t\bar{t}$ production. Smaller but still significant backgrounds come from W + jets and single top quark production. In the e + jets channel there is also a contribution from QCD multijet production. Other backgrounds have been found to be negligible. Data and SM background expectations agree in both shape and total normalization.

We apply a requirement of $S_T > 1240$ GeV in the final event selection. This condition is optimized to enhance the sensitivity to the signal, based on SM backgrounds and T signal expectations. The major selection requirements are summarized in Table VII.

Table VI (right columns) presents the event yields for expected SM backgrounds and data. Signal efficiencies are of the order of 0.5%–4% for T quark masses from 500 to 1000 GeV. They are summarized in Table VIII.

TABLE VII. Main selection requirements for the $T \to bW$ search with single leptons.

Variable	Selection
p_T muon	>45 GeV
p_T electron	>30 GeV
Number of jets	≥ 4
p_T jets	>120, 90, 50, and 30 GeV
W tags	0 or 1
b tags	1 or 2
S_T	>1240 GeV
E_T^{miss}	>30 GeV

TABLE VIII. Selection efficiencies and numbers of expected signal events for the selection $S_T > 1240$ GeV, for the two channels of the $T \to bW$ search with single leptons. Different T quark mass hypotheses are considered and a 100% branching fraction to bW is assumed.

	Muon channel		Electron channel	
T quark mass (GeV)	Efficiency	Events	Efficiency	Events
500	0.50%	59	0.46%	53
600	1.24%	43	1.30%	44
700	2.38%	28	2.38%	27
800	3.04%	13	3.17%	13
900	3.48%	5.6	3.63%	5.8
1000	3.52%	2.3	3.86%	2.5

The M_{fit} distribution for the final event selection is shown in Fig. 3. The μ + jets and e + jets final states give very similar results. The observed data are compatible with background expectations from SM processes. The μ + jets and e + jets channels are combined to improve the statistics for the simulated SM backgrounds.

C. All-hadronic search for $T \to tH$

This channel is optimized for the event topology in which at least one T quark decays to $T \to tH$, where the top quark decays into bW and the W boson decays

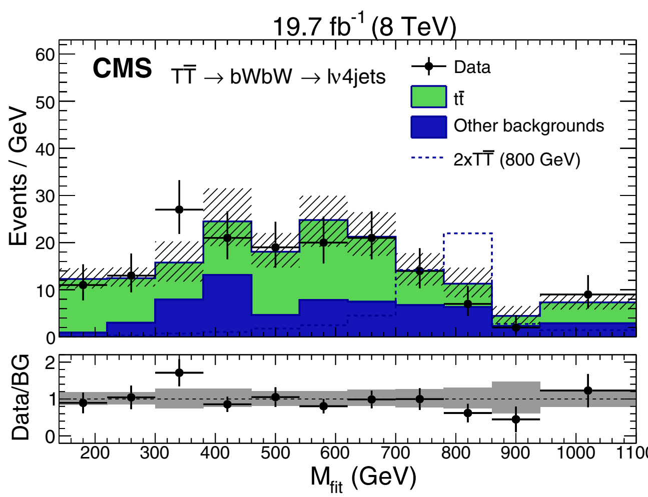

FIG. 3. Distributions of the reconstructed T quark mass M_{fit} for $bWbW$ candidate events in the search for $T \to bW$ with single leptons, combining the μ + jets and e + jets samples after the selection $S_T > 1240$ GeV. Data are shown as points and the simulated backgrounds as shaded histograms. The hatched region and the shaded area in the lower panel represent both the statistical and the systematic uncertainties in the total background. The expected signal for a T quark of mass 800 GeV is multiplied by a factor of 2. The lower panel represents the ratio between data and the sum of the backgrounds (BG). The horizontal error bars represent the bin width. The overflow of the distribution is added to the last bin.

TABLE IX. Main selection requirements for the all-hadronic search for $T \to tH$.

Variable	Selection
H_T^{sub}	>720 GeV
Number of CA15 jets	≥2
p_T CA15 jets	>150 GeV
p_T t-tagged jets	>200 GeV
Number of t tags	≥1
Number of H tags	≥1

hadronically, and the Higgs boson decays into two b quarks. Because of the expected high mass of the T quarks, the top quarks and Higgs bosons can have significant Lorentz boost; therefore the event selection is based on jet substructure requirements, as described in Sec. IVA.

At least one t-tagged and one H-tagged CA15 jet are required, where the t-tagged jets must have $p_T > 200$ GeV and the H-tagged jets must have $p_T > 150$ GeV. Two variables are used to further distinguish the signal from the background events after the event selection. These variables are H_T^{sub}, defined here as the scalar p_T sum of subjets of CA15 jets, and the invariant mass $m_{b\bar{b}}$ of two b-tagged subjets in the H-tagged jets. These two variables are used for setting upper limits on the T quark production cross section. The major selection requirements are summarized in Table IX.

Backgrounds due to QCD multijet production are determined from data using signal-depleted sideband regions. These sidebands are defined by inverting the jet substructure criteria. Backgrounds due to $t\bar{t}$ events are determined from simulation; other backgrounds are found to be negligible.

To maximize the sensitivity of the analysis, the events are divided into two categories: a category with a single H tag and a category with at least two H tags. The background estimates are well matched to the observed data, as discussed in Ref. [19]. For the final event selection, the H_T^{sub} and $m_{b\bar{b}}$ variables are combined into a single discriminator using a likelihood ratio method. The numbers of expected background events and events observed in data after the full selection are shown in Table X. The observed data are compatible with background expectations from SM processes. The signal selection efficiencies are between 2.5% and 7.2% which corresponds to an expected number of 283 signal events for a T quark mass of 500 GeV and 4.9 events for a T quark mass of 1000 GeV, assuming $\mathcal{B}(T \to tH) = 100\%$. A detailed table with selection efficiencies and expected numbers of signal events is available in Ref. [19].

TABLE X. Predicted numbers of total background events and observed events for the two event categories with one and with multiple H tags, for the all-hadronic search for $T \to tH$. The quoted uncertainties are statistical only. From Ref. [19].

	Single H tag category	Multiple H tags category
Total background	1403 ± 14	182 ± 5
Data	1355	205

D. All-hadronic search for $T \to bW$

This channel is optimized for the event topology in which both T quarks decay to $T \to bW$, where the W bosons decay hadronically. Events are selected by requiring two W-tagged CA8 jets with $p_T > 150$ GeV. At least two additional AK5 jets with $p_T > 50$ GeV are required, one of which must be b-tagged. Events are divided into categories defined by the numbers of b-tagged jets: one or at least two.

After the event selection, two T candidates T_1 and T_2 are reconstructed using combinations of the W jets and the AK5 jets. The order of T_1 and T_2 is arbitrary. The reconstruction is performed by identifying the combinations of W jets and AK5 jets having the smallest invariant mass difference. Figure 4 shows the two-dimensional distribution of the masses of each reconstructed T candidate in a signal sample with a simulated T quark mass of 800 GeV. The reconstructed mass peak is clearly visible at the expected value. The misreconstruction rate, where the wrong combination of jets is chosen, is small and does not affect the signal acceptance. Additional event requirements are then applied to increase sensitivity to the signal process. The T candidate masses must be greater than 200 GeV, and the fractional difference a_f in the masses of the two T candidates $m(T_1)$ and $m(T_2)$, where $a_f = |m(T_1) - m(T_2)|/(m(T_1) + m(T_2))$, must be less than 10%. The two T

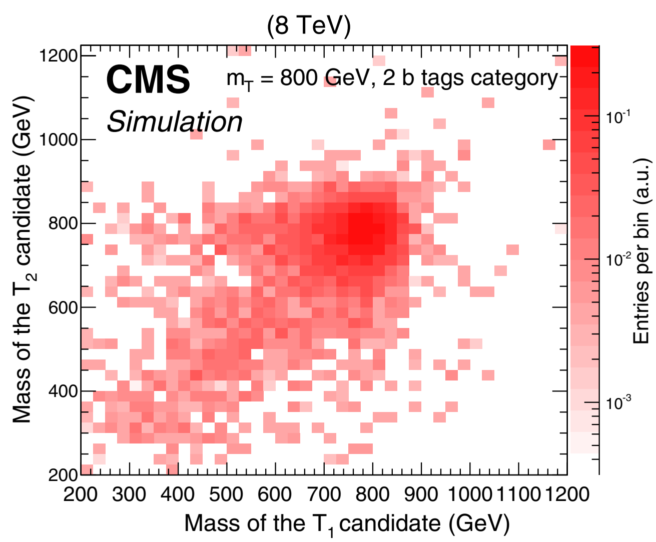

FIG. 4. Two-dimensional distribution of the masses of each reconstructed T candidate in the selected events for the all-hadronic search for $T \to bW$, for a simulated signal sample with a T quark mass of 800 GeV. The order of T_1 and T_2 is arbitrary.

TABLE XI. Main selection requirements for the all-hadronic search for $T \to bW$.

Variable	Selection
Number of AK5 jets	≥ 2
p_T AK5 jets	> 50 GeV
Number of W-tagged jets	≥ 2
p_T W-tagged jets	> 150 GeV
Reconstructed T candidate mass	> 200 GeV
a_f	$< 10\%$
$\Delta\phi(T_1, T_2)$	$> 5\pi/6$
H_T^{4jet}	> 1000 GeV

candidates must fall in opposite hemispheres of the detector, $\Delta\phi(T_1, T_2) > 5\pi/6$, and finally H_T^{4jet} must be above 1000 GeV, where H_T^{4jet} is defined as the scalar p_T sum of the four jets used to reconstruct the T candidates. The major selection requirements are summarized in Table XI.

The dominant backgrounds are due to QCD multijet production and $t\bar{t}$ production. Other background contributions are negligible.

To obtain the shape of the QCD multijet background, a control region is defined by requiring $H_T^{4jet} > 1000$ GeV, but inverting the requirement on the fractional mass difference, $a_f > 0.1$. This control region is enriched in multijet events and has a negligible signal contamination. The shape of the H_T^{4jet} distribution in the control region, after subtracting the expected $t\bar{t}$ contribution, is used to model the QCD multijet events entering the signal region. The H_T^{4jet} distribution in the signal region agrees with the distribution in the sideband region for simulated QCD multijet events. The normalization of the QCD multijet background is not fixed, and is determined in the limit setting procedure. This procedure is done independently for events containing one and at least two b-tagged jets.

Figure 5 shows the post-fit H_T^text4jet distributions obtained with the above method. Data are found to be in agreement with the expected background contributions. The numbers of expected background events and events observed in data after full selection are shown in Table XII. The numbers of expected signal events and selection efficiencies assuming $\mathcal{B}(T \to bW) = 100\%$ are summarized in Table XIII.

E. Search for $T \to tH$ with $H \to \gamma\gamma$

The analysis described in this section is optimized for events with one T quark decaying to tH, where the Higgs boson decays into a pair of photons. The main advantage of this channel is the possibility to precisely measure the invariant mass of the diphoton system ($m_{\gamma\gamma}$) so that a peak in the $m_{\gamma\gamma}$ distribution would be present for signal events. The disadvantage is the small Higgs branching fraction of the order of 2×10^{-3} [55]. The analysis concept is the same as for searches of the SM Higgs boson in the $H \to \gamma\gamma$ decay channel [56].

Events with two isolated photons are selected. Additional leptons and jets coming from the decay of top quarks or a second Higgs boson are required. In order to maximize the sensitivity of the analysis, two search channels are defined, targeting different decay modes of the top quark:

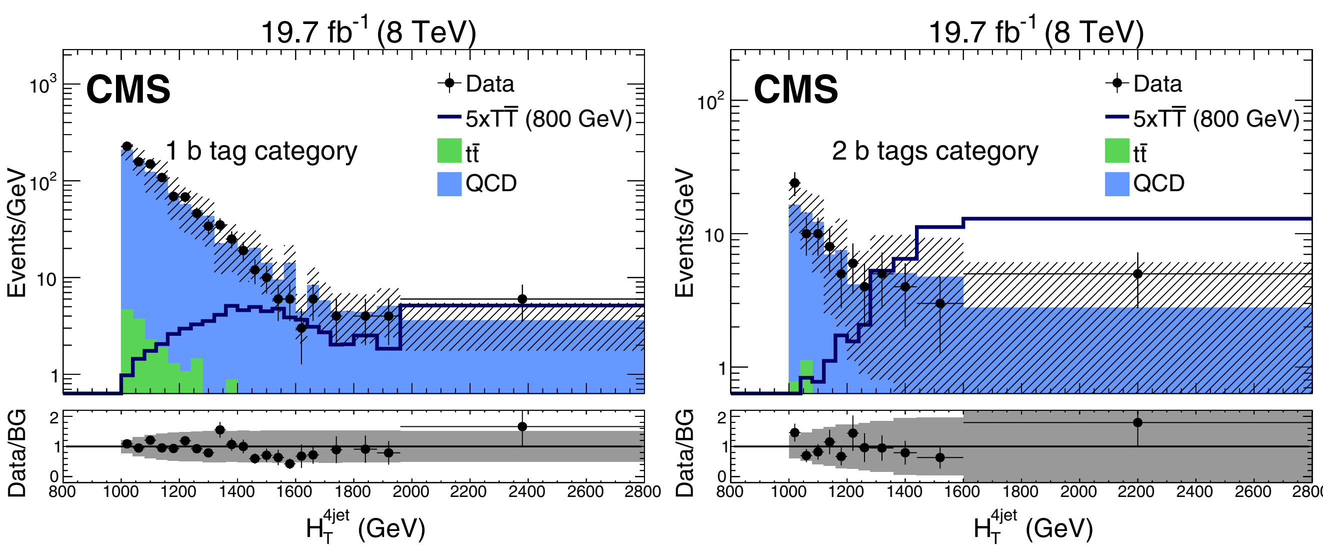

FIG. 5. The H_T^{4jet} distributions for single b tag events (left) and for events with at least two b tags (right) for the all-hadronic search for $T \to bW$, including the QCD multijet background estimate obtained from data and the T quark signal with a mass of 800 GeV. The hatched region and the shaded area in the lower panel represent both the statistical and the systematic uncertainties in the total background. The lower panel represents the ratio between data and the sum of the backgrounds (BG). The horizontal error bars represent the bin width.

TABLE XII. Summary of expected and observed background yields for the two channels of the $T \to bW$ search in the all-hadronic final state.

	1 b tag channel	$\geq 2b$ tags channel
$t\bar{t}$	20.3 ± 1.3	3.45 ± 0.55
QCD multijet	979 ± 29	80.2 ± 6.4
Total background	999 ± 31	84 ± 7
Data	998	84

TABLE XIII. Selection efficiencies and numbers of expected signal events, for the two channels of the $T \to bW$ search in the hadronic final state. Different T quark mass hypotheses are considered and a 100% branching fraction to bW is assumed.

T quark mass (GeV)	1 b tag channel		$\geq 2b$ tags channel	
	Efficiency	Events	Efficiency	Events
500	1.01%	103.4	0.86%	84.7
600	2.24%	66.0	1.81%	52.5
700	3.15%	31.24	2.35%	22.80
800	4.07%	14.64	2.51%	8.79
900	4.68%	6.57	2.44%	3.33
1000	4.95%	2.81	2.35%	1.29

(i) the leptonic channel searches for events with a pair of photons and at least one isolated high-p_T muon or electron;

(ii) the hadronic channel searches for events with a pair of photons and no isolated muons or electrons.

The resonant contributions from the $t\bar{t}H$ background are determined from simulation. The nonresonant contribution is composed of events with two prompt photons arising from QCD multijet production as well as for emission in top quark production ($\gamma\gamma +$ jets, $t\bar{t} + \gamma\gamma$, $t + \gamma\gamma$). The $t\bar{t}$ events are more likely to have a jet misreconstructed as a photon, because of the large numbers of jets in the final state. The simulation of such sources of instrumental background is not completely reliable. The background model is therefore derived from data.

The control sample used to estimate the nonresonant background consists of events where at least one photon passes loose identification requirements but does not pass the final event selection. This sample is enriched with events containing one misidentified photon. A reweighting is applied, in order to match the p_T and η spectra of the photons in this control sample to those obtained after the signal selection. This is done independently for each photon.

The event selection is based upon six quantities that have the largest discriminating powers between signal and backgrounds and that have small correlations. They include the transverse momenta of the larger p_T photon (γ_1) and smaller p_T photon (γ_2). The selection criteria are optimized to produce the most stringent limits on the signal cross

TABLE XIV. Final selection criteria for hadronic and leptonic channels of the search for $T \to tH$ with $H \to \gamma\gamma$.

Variable	Leptonic channel	Hadronic channel
$p_T(\gamma_1)$	$> \frac{1}{2} m_{\gamma\gamma}$	$> \frac{3}{4} m_{\gamma\gamma}$
$p_T(\gamma_2)$	25 GeV	35 GeV
Number of jets	≥ 2	≥ 2
S_T	≥ 770 GeV	≥ 1000 GeV
Leptons	≥ 1	0
b tags	⋯	≥ 1

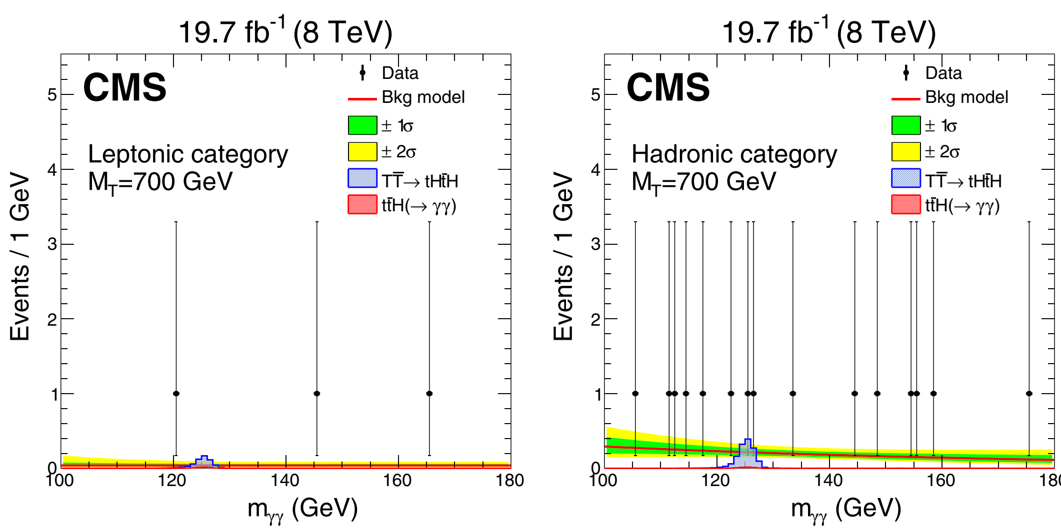

FIG. 6. Diphoton invariant mass distribution for the leptonic (left) and hadronic (right) channels of the search for $T \to tH$ with $H \to \gamma\gamma$. The signal is normalized to the predicted theoretical cross section corresponding to $m_T = 700$ GeV. The backgrounds predicted by the fit are shown as a solid line while the corresponding uncertainties are shown as bands around the line, where the inner band indicates the 1σ and the outer band indicates the 2σ uncertainties. Bins with zero entries are not shown.

TABLE XV. Expected yields for $t\bar{t}H$ and nonresonant background (from the fit to data) and the numbers of observed events in data after full event selection for the two channels of the $T \to tH$ search in the final state with photons. All the yields are computed in a window of 1 full width at half maximum i.e., 125 ± 1.5 GeV.

	Leptonic channel	Hadronic channel
$t\bar{t}H$	$0.039^{+0.005}_{-0.006}$	$0.042^{+0.005}_{-0.006}$
Nonresonant background	$0.11^{+0.07}_{-0.03}$	$0.65^{+0.16}_{-0.13}$
Total background	$0.15^{+0.07}_{-0.03}$	$0.69^{+0.16}_{-0.13}$
Data	0	2

TABLE XVI. Selection efficiencies and numbers of expected signal events, for the two channels of the $T \to tH$ search in the final state with photons. Different T quark mass hypotheses are considered and a 100% branching fraction to tH is assumed.

T quark mass (GeV)	Leptonic channel		Hadronic channel	
	Efficiency	Events	Efficiency	Events
500	6.7%	6.0	9.3%	8.3
600	9.6%	8.7	18.1%	16.4
700	11.0%	9.8	26.0%	23.8
800	12.0%	10.9	30.0%	27.3
900	11.4%	10.4	32.0%	29.3

section and are listed Table XIV for both leptonic and hadronic channels.

The nonresonant background contributions are obtained from unbinned maximum likelihood fits to the diphoton mass distribution over the range $100 < m_{\gamma\gamma} < 180$ GeV, under the hypothesis of no signal. An exponential function is chosen for these fits. Studies of pseudoexperiments showed that the use of an exponential function does not introduce a bias in the estimation of the numbers of background events in both categories. In Fig. 6, the observed diphoton mass distribution in each event category is shown, together with the expected signal and the expected resonant background contribution. The error bands show the uncertainty in the background shapes associated with the statistical uncertainties of the fits. The numbers of expected background events and events observed in data after final selection are shown in Table XV. The numbers of expected signal events and selection efficiencies assuming $\mathcal{B}(T \to tH) = 100\%$ are summarized in Table XVI.

The data in the signal window are compatible with background expectations from SM processes.

VI. COMBINATION STRATEGY

The event samples selected by the five analyses are almost entirely distinct and therefore, signal limits extracted from those analyses are statistically independent. They can be combined to yield a result that is more stringent than any of the inputs. Because the backgrounds are largely common to all analyses, the background estimates are largely correlated but well determined by the multiple independent samples. In particular, most analyses have top quark pair production as a background process. This background normalization is correlated among the analyses in the combination, providing for the combination a better background estimation than in the individual analyses. Similar arguments hold for the

TABLE XVII. Correlated and uncorrelated systematic uncertainties. The $\checkmark$ symbol indicates that the uncertainty has been taken into account in the analysis, but it is not correlated with any of the other analyses. The $\boxed{\checkmark}$ symbol indicates that the uncertainty has been taken into account and that it is correlated with the other analysis that have a $\boxed{\checkmark}$ sign as well. A missing symbol indicates that this uncertainty is not relevant for this analysis channel.

Uncertainty	Single leptons	Inclusive leptons	Multiple leptons	All-had. $T \to bW$	All-had. $T \to tH$	$H \to \gamma\gamma$
Int. luminosity	$\boxed{\checkmark}$	$\boxed{\checkmark}$	$\boxed{\checkmark}$	$\boxed{\checkmark}$	$\boxed{\checkmark}$	$\boxed{\checkmark}$
Trigger	$\checkmark$	$\checkmark$	$\checkmark$		$\checkmark$	$\checkmark$
Lepton ID	$\boxed{\checkmark}$	$\boxed{\checkmark}$	$\boxed{\checkmark}$			$\boxed{\checkmark}$
Photon ID						$\checkmark$
Photon energy						$\checkmark$
Pileup jet ID						$\checkmark$
Jet energy scale	$\boxed{\checkmark}$	$\boxed{\checkmark}$	$\boxed{\checkmark}$	$\boxed{\checkmark}$	$\boxed{\checkmark}$	$\boxed{\checkmark}$
Jet energy resolution	$\boxed{\checkmark}$	$\boxed{\checkmark}$	$\boxed{\checkmark}$	$\boxed{\checkmark}$	$\boxed{\checkmark}$	$\boxed{\checkmark}$
Unclustered energy	$\checkmark$					
b tag SF	$\boxed{\checkmark}$	$\boxed{\checkmark}$	$\boxed{\checkmark}$	$\boxed{\checkmark}$	$\boxed{\checkmark}$	
b tag mistag SF	$\boxed{\checkmark}$				$\boxed{\checkmark}$	
t tagging SF					$\checkmark$	
$t\bar{t}$ μR and μF scale	$\boxed{\checkmark}$	$\boxed{\checkmark}$	$\boxed{\checkmark}$	$\boxed{\checkmark}$	$\boxed{\checkmark}$	
$t\bar{t}$ cross section	$\boxed{\checkmark}$	$\boxed{\checkmark}$	$\boxed{\checkmark}$	$\boxed{\checkmark}$	$\boxed{\checkmark}$	
$t\bar{t}$ PDF	$\boxed{\checkmark}$			$\boxed{\checkmark}$	$\boxed{\checkmark}$	
QCD background				$\checkmark$	$\checkmark$	
Other backgrounds	$\checkmark$	$\boxed{\checkmark}$	$\boxed{\checkmark}$	$\checkmark$		$\checkmark$

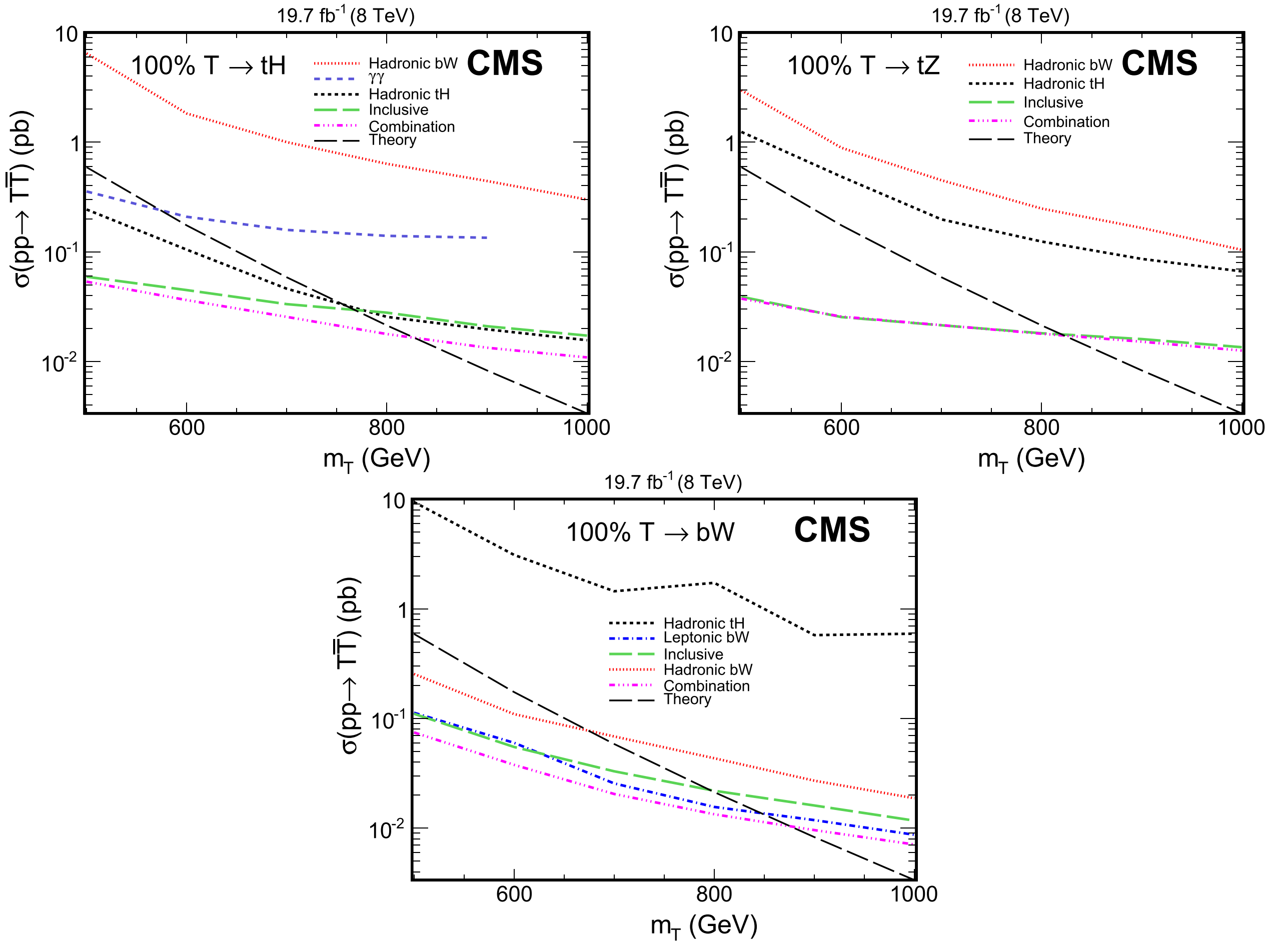

FIG. 7. Expected limits at 95% C.L. of the individual analyses in comparison to the combination for exclusive decays of the T quark to tH, tZ, and bW.

correlated systematic uncertainties, which are discussed in more detail in Sec. VI A.

The inclusive analysis with single and multiple leptons described in Sec. V A is able to set limits for all T quark decay modes. Dedicated optimizations to enhance the sensitivity for $T \to bW$ decays are described in Sec. V B. These optimizations use single-lepton events. To avoid double counting of events we replace the single-lepton part of the inclusive approach (Sec. V A) with the single-lepton analysis described in Sec. V B. This is done for scenarios with $\mathcal{B}(T \to bW)$ values of at least 80%. For lower $\mathcal{B}(T \to bW)$ values this approach is inferior and we use the inclusive results from Sec. V A only. At every point the approach used is that which gives the best expected limit. The other three analyses described in Secs. V C to V E do not have any overlap so they are always combined with the cases above.

For the statistical combination a Bayesian method [57] has been adopted in which the systematic uncertainties are taken into account as nuisance parameters with their corresponding priors as discussed in Sec. VI A. Upper limits on the T quark production cross section are obtained with the Theta framework [58]. Systematic uncertainties are taken into account as global normalization uncertainties and as shape uncertainties where applicable. More details about the treatment of systematic uncertainties are given in the next section.

A. Systematic uncertainties

Some of the individual analyses are sensitive to the same systematic uncertainties, for example the uncertainty in the integrated luminosity, the jet energy scale and the b tagging efficiency. Such uncertainties are treated as fully correlated, as is done technically by correlating the corresponding nuisance parameters in the limit setting procedure. This treatment allows improved constraints to be obtained on these parameters than is possible in the standard analyses.

The systematic uncertainties fall into two types: those which affect the normalization of the signal and background samples, and those which also affect the shapes of distributions. The uncertainty in the $t\bar{t}$ cross section is 13%. It is obtained from the $t\bar{t}$ cross section measurement [59] for large invariant mass values of the $t\bar{t}$ system. The uncertainty in the integrated luminosity is 2.6% [60].

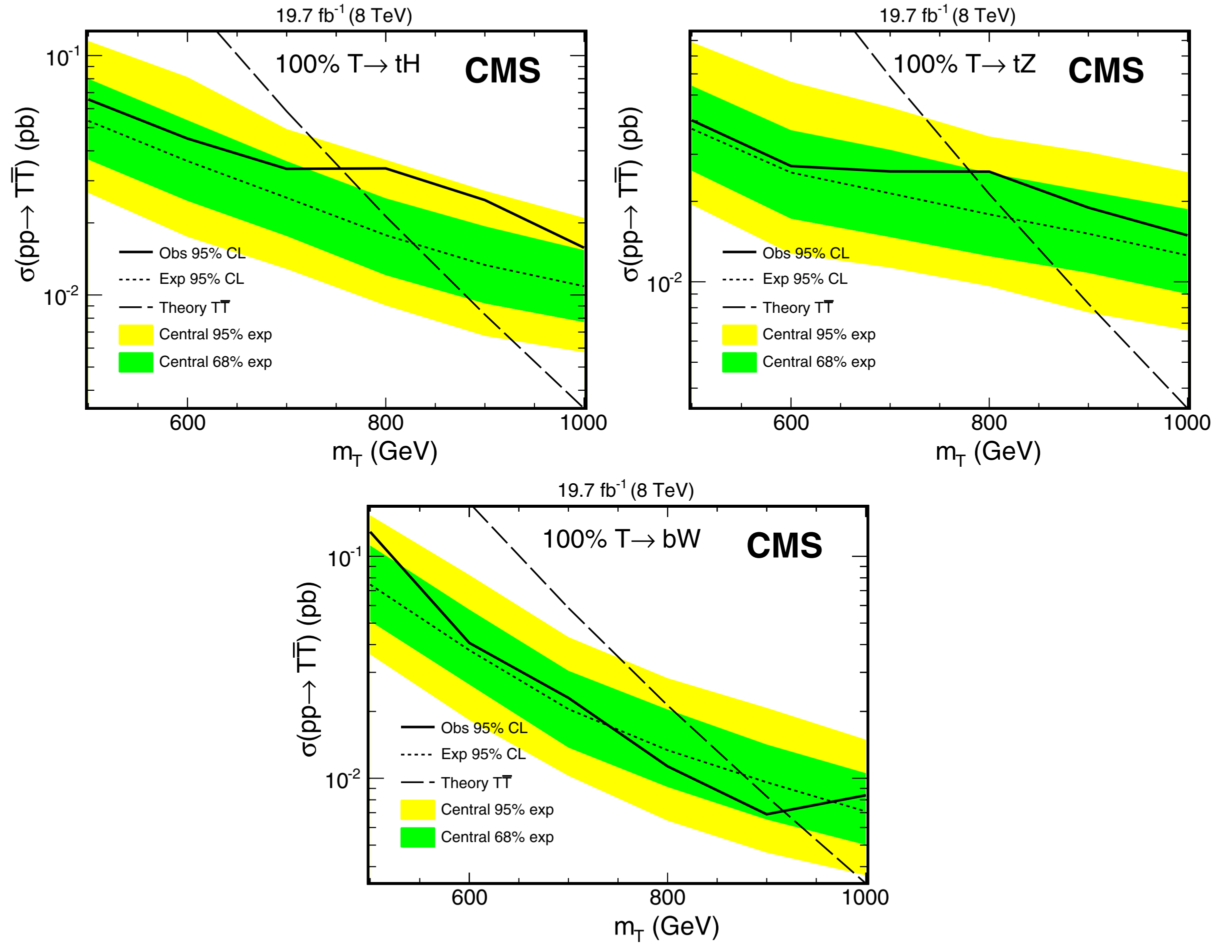

FIG. 8. Observed and expected Bayesian upper limits at 95% C.L. on the T quark production cross section for exclusive T quark decays to tH, tZ, and bW. The green (inner) and yellow (outer) bands show the 1σ (2σ) uncertainty ranges in the expected limits, respectively. The dashed line shows the prediction of the theory.

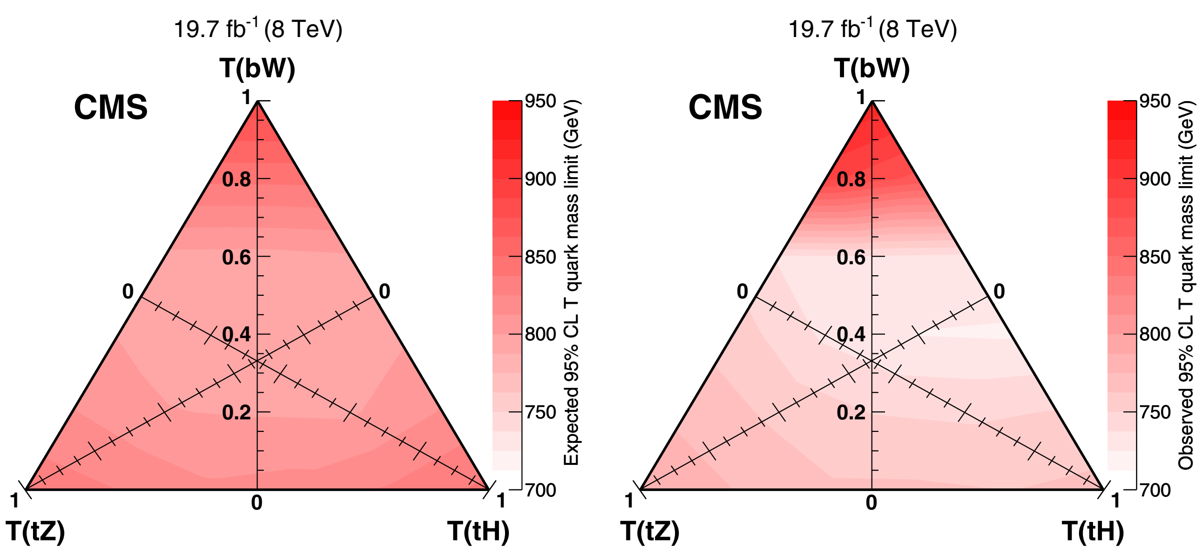

FIG. 9. Expected (left) and observed (right) 95% C.L. limits of the combined analysis, visualized in a triangle representing the branching fractions of the T quark decay.

TABLE XVIII. Branching fractions (first three columns) and the observed and expected upper limits on the T quark production cross section at 95% C.L. for different values of the T quark mass. The expected limits are quoted with their corresponding uncertainties, for different branching fractions hypotheses. The cross section limits are given in units of pb.

			T quark mass (GeV)					
$\mathcal{B}$ (tH)	$\mathcal{B}$ (tZ)	$\mathcal{B}$ (bW)	500	600	700	800	900	1000
0.0	1.0	0.0	$0.037^{+0.017}_{-0.011}$	$0.026^{+0.011}_{-0.009}$	$0.021^{+0.010}_{-0.006}$	$0.018^{+0.008}_{-0.006}$	$0.015^{+0.007}_{-0.004}$	$0.013^{+0.006}_{-0.004}$
			0.040	0.027	0.026	0.026	0.019	0.015
0.2	0.8	0.0	$0.043^{+0.022}_{-0.014}$	$0.029^{+0.013}_{-0.009}$	$0.023^{+0.012}_{-0.007}$	$0.019^{+0.009}_{-0.006}$	$0.016^{+0.008}_{-0.005}$	$0.013^{+0.005}_{-0.004}$
			0.045	0.030	0.031	0.030	0.023	0.016
0.4	0.6	0.0	$0.049^{+0.022}_{-0.016}$	$0.033^{+0.015}_{-0.011}$	$0.025^{+0.010}_{-0.008}$	$0.020^{+0.010}_{-0.006}$	$0.016^{+0.007}_{-0.005}$	$0.013^{+0.006}_{-0.004}$
			0.052	0.033	0.032	0.036	0.025	0.018
0.6	0.4	0.0	$0.053^{+0.025}_{-0.018}$	$0.035^{+0.015}_{-0.011}$	$0.026^{+0.012}_{-0.008}$	$0.020^{+0.009}_{-0.006}$	$0.016^{+0.006}_{-0.005}$	$0.013^{+0.005}_{-0.004}$
			0.066	0.038	0.033	0.035	0.024	0.017
0.8	0.2	0.0	$0.055^{+0.027}_{-0.018}$	$0.036^{+0.017}_{-0.011}$	$0.026^{+0.011}_{-0.009}$	$0.019^{+0.009}_{-0.006}$	$0.015^{+0.006}_{-0.005}$	$0.012^{+0.005}_{-0.004}$
			0.058	0.039	0.035	0.036	0.025	0.016
1.0	0.0	0.0	$0.053^{+0.027}_{-0.016}$	$0.036^{+0.018}_{-0.011}$	$0.025^{+0.011}_{-0.007}$	$0.018^{+0.007}_{-0.006}$	$0.013^{+0.006}_{-0.004}$	$0.011^{+0.004}_{-0.003}$
			0.066	0.045	0.034	0.034	0.025	0.016
0.0	0.8	0.2	$0.047^{+0.022}_{-0.014}$	$0.032^{+0.014}_{-0.010}$	$0.025^{+0.012}_{-0.007}$	$0.020^{+0.010}_{-0.006}$	$0.016^{+0.007}_{-0.005}$	$0.013^{+0.005}_{-0.004}$
			0.049	0.032	0.033	0.032	0.021	0.015
0.2	0.6	0.2	$0.056^{+0.029}_{-0.018}$	$0.036^{+0.018}_{-0.012}$	$0.027^{+0.013}_{-0.008}$	$0.021^{+0.011}_{-0.006}$	$0.016^{+0.008}_{-0.005}$	$0.013^{+0.006}_{-0.004}$
			0.055	0.037	0.038	0.035	0.026	0.016
0.4	0.4	0.2	$0.062^{+0.032}_{-0.020}$	$0.040^{+0.018}_{-0.012}$	$0.029^{+0.014}_{-0.009}$	$0.022^{+0.010}_{-0.007}$	$0.016^{+0.008}_{-0.004}$	$0.013^{+0.006}_{-0.004}$
			0.071	0.044	0.039	0.041	0.030	0.018
0.6	0.2	0.2	$0.068^{+0.035}_{-0.022}$	$0.043^{+0.022}_{-0.013}$	$0.031^{+0.013}_{-0.011}$	$0.022^{+0.010}_{-0.006}$	$0.016^{+0.007}_{-0.005}$	$0.012^{+0.006}_{-0.003}$
			0.080	0.053	0.039	0.042	0.026	0.018
0.8	0.0	0.2	$0.066^{+0.033}_{-0.021}$	$0.044^{+0.021}_{-0.014}$	$0.029^{+0.014}_{-0.009}$	$0.020^{+0.009}_{-0.006}$	$0.015^{+0.006}_{-0.005}$	$0.011^{+0.006}_{-0.003}$
			0.083	0.051	0.041	0.038	0.026	0.017
0.0	0.6	0.4	$0.061^{+0.033}_{-0.019}$	$0.039^{+0.018}_{-0.012}$	$0.030^{+0.013}_{-0.010}$	$0.021^{+0.010}_{-0.006}$	$0.017^{+0.006}_{-0.005}$	$0.012^{+0.006}_{-0.004}$
			0.071	0.042	0.039	0.036	0.023	0.015
0.2	0.4	0.4	$0.074^{+0.041}_{-0.024}$	$0.044^{+0.023}_{-0.013}$	$0.032^{+0.015}_{-0.010}$	$0.022^{+0.012}_{-0.006}$	$0.016^{+0.008}_{-0.004}$	$0.013^{+0.005}_{-0.004}$
			0.079	0.053	0.048	0.040	0.024	0.016
0.4	0.2	0.4	$0.082^{+0.048}_{-0.026}$	$0.050^{+0.023}_{-0.016}$	$0.034^{+0.015}_{-0.011}$	$0.023^{+0.010}_{-0.007}$	$0.017^{+0.007}_{-0.005}$	$0.012^{+0.005}_{-0.003}$
			0.102	0.061	0.052	0.041	0.028	0.015
0.6	0.0	0.4	$0.082^{+0.043}_{-0.024}$	$0.050^{+0.025}_{-0.015}$	$0.033^{+0.013}_{-0.011}$	$0.022^{+0.009}_{-0.007}$	$0.016^{+0.007}_{-0.005}$	$0.012^{+0.005}_{-0.004}$
			0.110	0.063	0.053	0.039	0.025	0.016
0.0	0.4	0.6	$0.082^{+0.042}_{-0.026}$	$0.048^{+0.023}_{-0.014}$	$0.033^{+0.016}_{-0.010}$	$0.022^{+0.010}_{-0.006}$	$0.016^{+0.008}_{-0.005}$	$0.011^{+0.006}_{-0.003}$
			0.093	0.057	0.049	0.038	0.022	0.014
0.2	0.2	0.6	$0.097^{+0.055}_{-0.032}$	$0.052^{+0.026}_{-0.016}$	$0.034^{+0.016}_{-0.010}$	$0.022^{+0.011}_{-0.006}$	$0.016^{+0.006}_{-0.005}$	$0.012^{+0.005}_{-0.004}$
			0.120	0.064	0.050	0.036	0.023	0.015
0.4	0.0	0.6	$0.102^{+0.052}_{-0.033}$	$0.053^{+0.028}_{-0.017}$	$0.034^{+0.014}_{-0.010}$	$0.022^{+0.009}_{-0.007}$	$0.015^{+0.007}_{-0.004}$	$0.011^{+0.005}_{-0.003}$
			0.129	0.072	0.049	0.039	0.024	0.015
0.0	0.2	0.8	$0.096^{+0.046}_{-0.030}$	$0.053^{+0.025}_{-0.017}$	$0.029^{+0.013}_{-0.009}$	$0.018^{+0.008}_{-0.006}$	$0.013^{+0.007}_{-0.004}$	$0.009^{+0.005}_{-0.002}$
			0.159	0.064	0.031	0.017	0.009	0.011
0.2	0.0	0.8	$0.104^{+0.055}_{-0.035}$	$0.054^{+0.027}_{-0.016}$	$0.029^{+0.015}_{-0.009}$	$0.018^{+0.009}_{-0.006}$	$0.013^{+0.007}_{-0.004}$	$0.011^{+0.004}_{-0.004}$
			0.215	0.072	0.038	0.018	0.010	0.014
0.0	0.0	1.0	$0.075^{+0.037}_{-0.024}$	$0.038^{+0.020}_{-0.012}$	$0.020^{+0.010}_{-0.006}$	$0.013^{+0.007}_{-0.004}$	$0.010^{+0.004}_{-0.003}$	$0.007^{+0.004}_{-0.002}$
			0.129	0.041	0.023	0.011	0.007	0.008

Shape uncertainties include the jet energy scale, the jet energy resolution and the b tagging efficiency uncertainties. We also consider the uncertainties in the efficiencies of the t tagging, W tagging, and H tagging algorithms [48,49,53]. The uncertainty due to the energy deposits not associated with jets (unclustered energy) has an impact on the missing p_{T}. This effect is taken into account in the single-lepton channel. The size of this uncertainty typically varies from a few percent up to 10%.

The systematic uncertainty in the pileup jet identification is taken into account in the analysis with $H \to \gamma\gamma$. It is derived through the use of the data/simulation scale factors (SF), which are binned in jet η and p_{T} [56].

For the photon identification efficiency, the uncertainty in the SF is taken into account. The SF corrects the efficiency in simulation to the efficiency as measured in data using a "tag-and-probe" technique [61] applied to $Z \to e^+e^-$ events. The uncertainty applied to this SF amounts to 3% in the barrel region of the calorimeter and 4% in the endcaps.

Lepton trigger efficiencies, lepton identification efficiencies, and corresponding correction factors for simulated events are obtained from data using decays of Z bosons to dileptons. These uncertainties are $\leq 3\%$.

For simulated $t\bar{t}$ and ttH events, uncertainties due to renormalization and factorization scales (μ_{R} and μ_{F}) are taken into account by varying both scales simultaneously up and down by a factor of two. Uncertainties arising from the choice of PDFs are taken into account. Simulated background events are weighted according to the uncertainties parametrized by the CTEQ6 eigenvectors [31]. The shifts produced by the individual eigenvectors are added in quadrature in each bin of the relevant distributions.

A systematic uncertainty of 50% is assigned to the diboson backgrounds, single top quark production and the W and Z boson background. This accounts for the effects of the μ_{R} and μ_{F} variations in simulation and the uncertainties in the determination of the $W+$jets SF from data.

Modified "template" distributions of those quantities that are affected by the respective uncertainties are obtained by varying the respective quantity by its uncertainty, namely by ± 1 standard deviation. In the limit setting procedure a likelihood fit is performed in which the nominal distribution and the modified templates are interpolated. The corresponding uncertainty is represented as a nuisance parameter, which receives its prior constraints from the template distributions. In the fit, the templates are allowed to be extrapolated beyond ± 1 standard deviation, but this happens rarely. The resulting fit values are always within ± 1.5 standard deviations of their prior values.

The list of nuisance parameters of all analysis channels is shown in Table XVII. This table also indicates which parameters are correlated and which uncorrelated.

VII. RESULTS

No significant deviation from the SM prediction is observed. The expected limits of the individual analysis channels at a 95% confidence level (C.L.) are displayed in Fig. 7 for exclusive decays of the T quark to tH, tZ,

TABLE XIX. Lower limits on the mass of the T quark at 95% C.L., for different combinations of T quark branching fractions. The 1σ uncertainty range on the expected limits are given as well.

$\mathcal{B}(tH)$	$\mathcal{B}(tZ)$	$\mathcal{B}(bW)$	Observed limit	Expected limit	Expected 1σ
0.0	1.0	0.0	790	830	[790, 880]
0.2	0.8	0.0	780	820	[780, 870]
0.4	0.6	0.0	760	810	[770, 870]
0.6	0.4	0.0	760	820	[770, 870]
0.8	0.2	0.0	760	830	[780, 880]
1.0	0.0	0.0	770	840	[780, 890]
0.0	0.8	0.2	770	810	[770, 870]
0.2	0.6	0.2	760	800	[760, 870]
0.4	0.4	0.2	750	800	[760, 870]
0.6	0.2	0.2	750	800	[760, 870]
0.8	0.0	0.2	750	810	[770, 880]
0.0	0.6	0.4	760	800	[760, 870]
0.2	0.4	0.4	730	800	[750, 860]
0.4	0.2	0.4	720	790	[740, 860]
0.6	0.0	0.4	720	800	[750, 870]
0.0	0.4	0.6	740	800	[750, 860]
0.2	0.2	0.6	740	800	[740, 870]
0.4	0.0	0.6	730	800	[750, 870]
0.0	0.2	0.8	890	840	[780, 890]
0.2	0.0	0.8	870	840	[770, 890]
0.0	0.0	1.0	920	890	[810, 950]

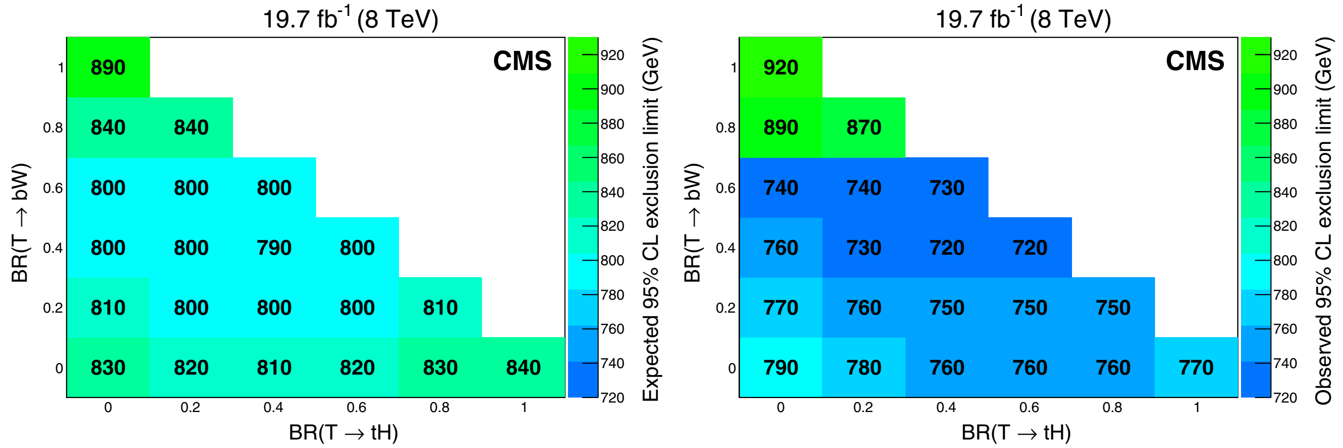

FIG. 10. Expected (left) and observed (right) 95% C.L. limits of the combined analysis, for combinations of branching fractions to tH, tZ, and bW. The branching fraction to tZ is not explicitly reported, since it is given by $1 - \mathcal{B}(tH) - \mathcal{B}(bW)$.

and bW. This figure also shows the result of the combination, where only the nonoverlapping part of the individual analyses are combined, as discussed in Sec. VI.

The observed limits and the expected one and two standard deviation uncertainties are displayed in Fig. 8 for exclusive T quark decays.

The lower limits on the mass of the T quark are obtained by determining the intersection between expected (observed) limits with the theoretical prediction, based on the cross section versus T quark mass distributions shown in Fig. 8. The results are visualized graphically in the triangular plane of branching fractions in Fig. 9. The numerical upper limits on the T quark production cross section are given in Table XVIII for a full range of branching fractions and the numerical results of the limits on the mass of the T quark are given in Table XIX. A different visualization of the mass limits is presented in Fig. 10.

Depending on the assumed branching fractions, the expected limits lie between 790 and 890 GeV, while the observed limits are in a range between 720 and 920 GeV. In much of the triangular plane of branching fractions these are the most stringent limits on T quark pair production to date.

VIII. SUMMARY

A search for pair production of vectorlike T quarks of charge 2/3 has been performed. In most models the hypothetical T quark has three decay modes: $T \to tH$, $T \to tZ$, and $T \to bW$. The following five distinct topologies have been investigated: inclusive lepton events covering all possible decay modes, single-lepton events optimized to find $T \to bW$ decays, all-hadronic events optimized either for $T \to tH$ or $T \to bW$ decays, and events containing a Higgs boson decaying to a pair of photons.

Data and SM background expectations are found to be in agreement. Upper limits on the production cross sections of vector-like T quarks are set. The expected 95% C.L. lower mass limits are between 790 and 890 GeV depending on the branching fraction of the T quark. For a branching fraction of $\mathcal{B}(tH) = 100\%$ an expected (observed) limit of 840 (770) GeV is found. For $\mathcal{B}(tZ) = 100\%$ the expected (observed) limit is 830 (790) GeV and for $\mathcal{B}(bW) = 100\%$ the limit is 890 (920) GeV. These are among the strongest limits on vectorlike T quarks obtained to date.

ACKNOWLEDGMENTS

We congratulate our colleagues in the CERN accelerator departments for the excellent performance of the LHC and thank the technical and administrative staffs at CERN and at other CMS institutes for their contributions to the success of the CMS effort. In addition, we gratefully acknowledge the computing centers and personnel of the Worldwide LHC Computing Grid for delivering so effectively the computing infrastructure essential to our analyses. Finally, we acknowledge the enduring support for the construction and operation of the LHC and the CMS detector provided by the following funding agencies: the Austrian Federal Ministry of Science, Research and Economy and the Austrian Science Fund; the Belgian Fonds de la Recherche Scientifique, and Fonds voor Wetenschappelijk Onderzoek; the Brazilian Funding Agencies (CNPq, CAPES, FAPERJ, and FAPESP); the Bulgarian Ministry of Education and Science; CERN; the Chinese Academy of Sciences, Ministry of Science and Technology, and National Natural Science Foundation of China; the Colombian Funding Agency (COLCIENCIAS); the Croatian Ministry of Science, Education and Sport, and the Croatian Science Foundation; the Research Promotion Foundation, Cyprus; the Ministry of Education and Research, Estonian Research Council via IUT23-4 and IUT23-6 and European Regional Development Fund, Estonia; the Academy of Finland, Finnish Ministry of Education and Culture; Helsinki Institute of Physics; the Institut National de Physique Nucléaire et de Physique des Particules / CNRS, and Commissariat à l'Énergie Atomique et aux Énergies Alternatives / CEA, France; the Bundesministerium für Bildung und Forschung, Deutsche Forschungsgemeinschaft, and Helmholtz-Gemeinschaft

Deutscher Forschungszentren, Germany; the General Secretariat for Research and Technology, Greece; the National Scientific Research Foundation, and National Innovation Office, Hungary; the Department of Atomic Energy and the Department of Science and Technology, India; the Institute for Studies in Theoretical Physics and Mathematics, Iran; the Science Foundation, Ireland; the Istituto Nazionale di Fisica Nucleare, Italy; the Ministry of Science, ICT and Future Planning, and National Research Foundation (NRF), Republic of Korea; the Lithuanian Academy of Sciences; the Ministry of Education, and University of Malaya (Malaysia); the Mexican Funding Agencies (CINVESTAV, CONACYT, SEP, and UASLP-FAI); the Ministry of Business, Innovation and Employment, New Zealand; the Pakistan Atomic Energy Commission; the Ministry of Science and Higher Education and the National Science Centre, Poland; the Fundação para a Ciência e a Tecnologia, Portugal; JINR, Dubna; the Ministry of Education and Science of the Russian Federation, the Federal Agency of Atomic Energy of the Russian Federation, Russian Academy of Sciences, and the Russian Foundation for Basic Research; the Ministry of Education, Science and Technological Development of Serbia; the Secretaría de Estado de Investigación, Desarrollo e Innovación and Programa Consolider-Ingenio 2010, Spain; the Swiss Funding Agencies (ETH Board, ETH Zurich, PSI, SNF, UniZH, Canton Zurich, and SER); the Ministry of Science and Technology, Taipei; the Thailand Center of Excellence in Physics, the Institute for the Promotion of Teaching Science and Technology of Thailand, Special Task Force for Activating Research and the National Science and Technology Development Agency of Thailand; the Scientific and Technical Research Council of Turkey, and Turkish Atomic Energy Authority; the National Academy of Sciences of Ukraine, and State Fund for Fundamental Researches, Ukraine; the Science and Technology Facilities Council, UK; the US Department of Energy, and the US National Science Foundation. Individuals have received support from the Marie-Curie programme and the European Research Council and EPLANET (European Union); the Leventis Foundation; the Alfred P. Sloan Foundation; the Alexander von Humboldt Foundation; the Belgian Federal Science Policy Office; the Fonds pour la Formation à la Recherche dans l'Industrie et dans l'Agriculture (FRIA-Belgium); the Agentschap voor Innovatie door Wetenschap en Technologie (IWT-Belgium); the Ministry of Education, Youth and Sports (MEYS) of the Czech Republic; the Council of Science and Industrial Research, India; the HOMING PLUS programme of the Foundation for Polish Science, cofinanced from European Union, Regional Development Fund; the Compagnia di San Paolo (Torino); the Consorzio per la Fisica (Trieste); MIUR project 20108T4XTM (Italy); the Thalis and Aristeia programmes cofinanced by EU-ESF and the Greek NSRF; the National Priorities Research Program by Qatar National Research Fund; the Rachadapisek Sompot Fund for Postdoctoral Fellowship, Chulalongkorn University (Thailand); and the Welch Foundation.

[1] ATLAS Collaboration, Observation of a new particle in the search for the standard model Higgs boson with the ATLAS detector at the LHC, Phys. Lett. B **716**, 1 (2012).

[2] CMS Collaboration, Observation of a new boson at a mass of 125 GeV with the CMS experiment at the LHC, Phys. Lett. B **716**, 30 (2012).

[3] CMS Collaboration, Observation of a new boson with mass near 125 GeV in pp collisions at $\sqrt{s} = 7$ and 8 TeV, J. High Energy Phys. 06 (2013) 081.

[4] N. Arkani-Hamed, A. G. Cohen, and H. Georgi, Electroweak symmetry breaking from dimensional deconstruction, Phys. Lett. B **513**, 232 (2001).

[5] M. Schmaltz and D. Tucker-Smith, Little Higgs review, Annu. Rev. Nucl. Part. Sci. **55**,229 (2005).

[6] I. Antoniadis, K. Benakli, and M. Quiros, Finite Higgs mass without supersymmetry, New J. Phys. **3**,20 (2001).

[7] Y. Hosotani, S. Noda, and K. Takenaga, Dynamical gauge-Higgs unification in the electroweak theory, Phys. Lett. B **607**, 276 (2005).

[8] K. Agashe, R. Contino, and A. Pomarol, The minimal composite Higgs model, Nucl. Phys. **B719**, 165 (2005).

[9] C. T. Hill and E. H. Simmons, Strong dynamics and electroweak symmetry breaking, Phys. Rep. **381**, 235 (2003).

[10] J. A. Aguilar-Saavedra, R. Benbrik, S. Heinemeyer, and M. Pérez-Victoria, Handbook of vector-like quarks: mixing and single production, Phys. Rev. D **88**, 094010 (2013).

[11] O. Eberhardt, G. Herbert, H. Lacker, A. Lenz, A. Menzel, U. Nierste, and M. Wiebusch, Joint analysis of Higgs boson decays and electroweak precision observables in the standard model with a sequential fourth generation, Phys. Rev. D **86**, 013011 (2012).

[12] CMS Collaboration, Search for pair produced fourth-generation up-type quarks in pp collisions at $\sqrt{s} = 7$ TeV with a lepton in the final state, Phys. Lett. B **718**, 307 (2012).

[13] CMS Collaboration, Search for heavy, top-like quark pair production in the dilepton final state in pp collisions at $\sqrt{s} = 7$ TeV, Phys. Lett. B **716**, 103 (2012).

[14] CMS Collaboration, Search for a Vectorlike Quark with Charge 2/3 in tZ Events from pp Collisions at $\sqrt{s} = 7$ TeV, Phys. Rev. Lett. **107**, 271802 (2011).

[15] CMS Collaboration, Inclusive search for a vector-like T quark with charge 2/3 in pp collisions at $\sqrt{s} = 8$ TeV, Phys. Lett. B **729**, 149 (2014).
[16] ATLAS Collaboration, Search for pair and single production of new heavy quarks that decay to a Z boson and a third-generation quark in pp collisions at $\sqrt{s} = 8$ TeV with the ATLAS detector, J. High Energy Phys. 11 (2014) 104.
[17] ATLAS Collaboration, Analysis of events with b-jets and a pair of leptons of the same charge in pp collisions at $\sqrt{s} = 8$ TeV with the ATLAS detector, J. High Energy Phys. 10 (2015) 150.
[18] ATLAS Collaboration, Search for production of vector-like quark pairs and of four top quarks in the lepton-plus-jets final state in pp collisions at $\sqrt{s} = 8$ TeV with the ATLAS detector, J. High Energy Phys. 08 (2015) 105.
[19] CMS Collaboration, Search for vector-like T quarks decaying to top quarks and Higgs bosons in the all-hadronic channel using jet substructure, J. High Energy Phys. 06 (2015) 080.
[20] CMS Collaboration, The CMS experiment at the CERN LHC, J. Instrum. **3**, S08004 (2008).
[21] CMS Collaboration, Performance of electron reconstruction and selection with the CMS detector in proton-proton collisions at $\sqrt{s} = 8$ TeV, J. Instrum. **10**, P06005 (2015).
[22] CMS Collaboration, Energy calibration and resolution of the CMS electromagnetic calorimeter in pp collisions at $\sqrt{s} = 7$ TeV, J. Instrum. **8**, P09009 (2013).
[23] CMS Collaboration, Description and performance of track and primary-vertex reconstruction with the CMS tracker, J. Instrum. **9**, P10009 (2014).
[24] P. Nason, A new method for combining NLO QCD with shower Monte Carlo algorithms, J. High Energy Phys. 11 (2004) 040.
[25] S. Frixione, P. Nason, and C. Oleari, Matching NLO QCD computations with parton shower simulations: the POWHEG method, J. High Energy Phys. 11 (2007) 070.
[26] S. Alioli, P. Nason, C. Oleari, and E. Re, A general framework for implementing NLO calculations in shower Monte Carlo programs: the POWHEG BOX, J. High Energy Phys. 06 (2010) 043.
[27] J. Alwall, M. Herquet, F. Maltoni, O. Mattelaer, and T. Stelzer, MadGraph 5: Going beyond, J. High Energy Phys. 06 (2011) 128.
[28] T. Sjöstrand, S. Mrenna, and P. Z. Skands, PYTHIA 6.4 Physics and Manual, J. High Energy Phys. 05 (2006) 026.
[29] J. Alwall, S. Höche, F. Krauss, N. Lavesson, L. Lönnblad, F. Maltoni, M. L. Mangano, M. Moretti, C. G. Papadopoulos, F. Piccinini, S. Schumann, M. Treccani, J. Winter, and M. Worek, Comparative study of various algorithms for the merging of parton showers and matrix elements in hadronic collisions, Eur. Phys. J. C **53**, 473 (2008).
[30] J. Alwall, S. Visscher, and F. Maltoni, QCD radiation in the production of heavy colored particles at the LHC, J. High Energy Phys. 02 (2009) 017.
[31] J. Pumplin, D. R. Stump, J. Huston, H.-Liang Lai, P. Nadolsky, and Wu-Ki Tung, New generation of parton distributions with uncertainties from global QCD analysis, J. High Energy Phys. 07 (2002) 012.
[32] M. Czakon, P. Fiedler, and A. Mitov, The Total Top Quark Pair Production Cross-Section at Hadron Colliders through $O(\alpha_S^4)$, Phys. Rev. Lett. **110**, 252004 (2013).
[33] M. Czakon and A. Mitov, Top++: A program for the calculation of the top-pair cross-section at hadron colliders, Comput. Phys. Commun. **185**, 2930 (2014).
[34] K. Rose, Deterministic annealing for clustering, compression, classification, regression and related optimisation problems, Proc. IEEE **86**, 2210 (1998).
[35] W. Waltenberger, R. Früwirth, and P. Vanlaer, Adaptive vertex fitting, J. Phys. G **34**, N343 (2007).
[36] CMS Collaboration, CMS Physics Analysis Summary Report No. CMS-PAS-PFT-09-001, http://cdsweb.cern.ch/record/1194487, 2009.
[37] CMS Collaboration, CMS Physics Analysis Summary Report No. CMS-PAS-PFT-10-001, http://cdsweb.cern.ch/record/1247373, 2010.
[38] CMS Collaboration, Performance of photon reconstruction and identification with the CMS detector in proton-proton collisions at $\sqrt{s} = 8$ TeV, J. Instrum. **10**, P08010 (2015).
[39] M. Cacciari, G. P. Salam, and G. Soyez, The anti-k_t jet clustering algorithm, J. High Energy Phys. 04 (2008) 063.
[40] M. Cacciari, G. P. Salam, and G. Soyez, Fastjet user manual, Eur. Phys. J. C **72**, 1896 (2012).
[41] Y. L. Dokshitzer, G. D. Leder, S. Moretti, and B. R. Webber, Better jet clustering algorithms, J. High Energy Phys. 08 (1997) 001.
[42] CMS Collaboration, Determination of jet energy calibration and transverse momentum resolution in CMS, J. Instrum. **6**, P11002 (2011).
[43] M. Cacciari, G. P. Salam, and G. Soyez, The catchment area of jets, J. High Energy Phys. 04 (2008) 005.
[44] CMS Collaboration, Identification of b-quark jets with the CMS experiment, J. Instrum. **8**, P04013 (2013).
[45] CMS Collaboration, Search for anomalous $t\bar{t}$ production in the highly-boosted all-hadronic final state, J. High Energy Phys. 09 (2012) 029.
[46] D. E. Kaplan, K. Rehermann, M. D. Schwartz, and B. Tweedie, Top Tagging: A Method for Identifying Boosted Hadronically Decaying Top Quarks, Phys. Rev. Lett. **101**, 142001 (2008).
[47] T. Plehn and M. Spannowsky, Top tagging, J. Phys. G **39**, 083001 (2012).
[48] CMS Collaboration, CMS Physics Analysis Summary Report No. CMS-PAS-JME-13-007, http://cds.cern.ch/record/1647419, 2013.
[49] CMS Collaboration, CMS Physics Analysis Summary Report No. CMS-PAS-BTV-13-001, http://cds.cern.ch/record/1581306, 2013.
[50] J. M. Butterworth, A. R. Davison, M. Rubin, and G. P. Salam, Jet Substructure as a New Higgs Search Channel at the LHC, Phys. Rev. Lett. **100**, 242001 (2008).
[51] S. D. Ellis, C. K. Vermilion, and J. R. Walsh, Techniques for improved heavy particle searches with jet substructure, Phys. Rev. D **80**, 051501 (2009).
[52] S. D. Ellis, C. K. Vermilion, and J. R. Walsh, Recombination algorithms and jet substructure: pruning as a tool for heavy particle searches, Phys. Rev. D **81**, 094023 (2010).
[53] CMS Collaboration, Identification techniques for highly boosted W bosons that decay into hadrons, J. High Energy Phys. 12 (2014) 017.
[54] H. Voss, A. Höcker, J. Stelzer, and F. Tegenfeldt, TMVA, the toolkit for multivariate data analysis with ROOT, *Proc. Sci.*, ACAT2007 (2007) 040 [arXiv:physics/0703039].

[55] J. R. Andersen et al. (LHC Higgs Cross Section Working Group), Handbook of LHC Higgs Cross Sections: 3. Higgs Properties, 2013.
[56] CMS Collaboration, Observation of the diphoton decay of the Higgs boson and measurement of its properties, Eur. Phys. J. C 74, 3076 (2014).
[57] A. O'Hagan and J. Foster, *Kendalls Advanced Theory of Statistic 2B: Bayesian Inference* (Wiley, New York, 2010).
[58] J. Ott, http://www.theta-framework.org/.
[59] CMS Collaboration, Measurement of the differential cross section for top quark pair production in pp collisions at $\sqrt{s} = 8$ TeV, arXiv:1505.04480.
[60] CMS Collaboration, CMS Physics Analysis Summary Report No. CMS-PAS-LUM-13-001, http://cds.cern.ch/record/159886, 2013.
[61] CMS Collaboration, Measurement of the inclusive W and Z production cross sections in pp collisions at $\sqrt{s} = 7$ TeV with the CMS experiment, J. High Energy Phys. 10 (2011) 132.

V. Khachatryan,[1] A. M. Sirunyan,[1] A. Tumasyan,[1] W. Adam,[2] E. Asilar,[2] T. Bergauer,[2] J. Brandstetter,[2] E. Brondolin,[2] M. Dragicevic,[2] J. Erö,[2] M. Flechl,[2] M. Friedl,[2] R. Frühwirth,[2,b] V. M. Ghete,[2] C. Hartl,[2] N. Hörmann,[2] J. Hrubec,[2] M. Jeitler,[2,b] V. Knünz,[2] A. König,[2] M. Krammer,[2,b] I. Krätschmer,[2] D. Liko,[2] T. Matsushita,[2] I. Mikulec,[2] D. Rabady,[2,c] B. Rahbaran,[2] H. Rohringer,[2] J. Schieck,[2,b] R. Schöfbeck,[2] J. Strauss,[2] W. Treberer-Treberspurg,[2] W. Waltenberger,[2] C.-E. Wulz,[2,b] V. Mossolov,[3] N. Shumeiko,[3] J. Suarez Gonzalez,[3] S. Alderweireldt,[4] T. Cornelis,[4] E. A. De Wolf,[4] X. Janssen,[4] A. Knutsson,[4] J. Lauwers,[4] S. Luyckx,[4] R. Rougny,[4] M. Van De Klundert,[4] H. Van Haevermaet,[4] P. Van Mechelen,[4] N. Van Remortel,[4] A. Van Spilbeeck,[4] S. Abu Zeid,[5] F. Blekman,[5] J. D'Hondt,[5] N. Daci,[5] I. De Bruyn,[5] K. Deroover,[5] N. Heracleous,[5] J. Keaveney,[5] S. Lowette,[5] L. Moreels,[5] A. Olbrechts,[5] Q. Python,[5] D. Strom,[5] S. Tavernier,[5] W. Van Doninck,[5] P. Van Mulders,[5] G. P. Van Onsem,[5] I. Van Parijs,[5] P. Barria,[6] H. Brun,[6] C. Caillol,[6] B. Clerbaux,[6] G. De Lentdecker,[6] G. Fasanella,[6] L. Favart,[6] A. Grebenyuk,[6] G. Karapostoli,[6] T. Lenzi,[6] A. Léonard,[6] T. Maerschalk,[6] A. Marinov,[6] L. Perniè,[6] A. Randle-conde,[6] T. Reis,[6] T. Seva,[6] C. Vander Velde,[6] P. Vanlaer,[6] R. Yonamine,[6] F. Zenoni,[6] F. Zhang,[6,d] K. Beernaert,[7] L. Benucci,[7] A. Cimmino,[7] S. Crucy,[7] D. Dobur,[7] A. Fagot,[7] G. Garcia,[7] M. Gul,[7] J. Mccartin,[7] A. A. Ocampo Rios,[7] D. Poyraz,[7] D. Ryckbosch,[7] S. Salva,[7] M. Sigamani,[7] N. Strobbe,[7] M. Tytgat,[7] W. Van Driessche,[7] E. Yazgan,[7] N. Zaganidis,[7] S. Basegmez,[8] C. Beluffi,[8,e] O. Bondu,[8] S. Brochet,[8] G. Bruno,[8] R. Castello,[8] A. Caudron,[8] L. Ceard,[8] G. G. Da Silveira,[8] C. Delaere,[8] D. Favart,[8] L. Forthomme,[8] A. Giammanco,[8,f] J. Hollar,[8] A. Jafari,[8] P. Jez,[8] M. Komm,[8] V. Lemaitre,[8] A. Mertens,[8] C. Nuttens,[8] L. Perrini,[8] A. Pin,[8] K. Piotrzkowski,[8] A. Popov,[8,g] L. Quertenmont,[8] M. Selvaggi,[8] M. Vidal Marono,[8] N. Beliy,[9] G. H. Hammad,[9] W. L. Aldá Júnior,[10] G. A. Alves,[10] L. Brito,[10] M. Correa Martins Junior,[10] M. Hamer,[10] C. Hensel,[10] C. Mora Herrera,[10] A. Moraes,[10] M. E. Pol,[10] P. Rebello Teles,[10] E. Belchior Batista Das Chagas,[11] W. Carvalho,[11] J. Chinellato,[11,h] A. Custódio,[11] E. M. Da Costa,[11] D. De Jesus Damiao,[11] C. De Oliveira Martins,[11] S. Fonseca De Souza,[11] L. M. Huertas Guativa,[11] H. Malbouisson,[11] D. Matos Figueiredo,[11] L. Mundim,[11] H. Nogima,[11] W. L. Prado Da Silva,[11] A. Santoro,[11] A. Sznajder,[11] E. J. Tonelli Manganote,[11,h] A. Vilela Pereira,[11] S. Ahuja,[12a] C. A. Bernardes,[12b] A. De Souza Santos,[12b] S. Dogra,[12a] T. R. Fernandez Perez Tomei,[12a] E. M. Gregores,[12b] P. G. Mercadante,[12b] C. S. Moon,[12a,i] S. F. Novaes,[12a] Sandra S. Padula,[12a] D. Romero Abad,[12a] J. C. Ruiz Vargas,[12a] A. Aleksandrov,[13] R. Hadjiiska,[13] P. Iaydjiev,[13] M. Rodozov,[13] S. Stoykova,[13] G. Sultanov,[13] M. Vutova,[13] A. Dimitrov,[14] I. Glushkov,[14] L. Litov,[14] B. Pavlov,[14] P. Petkov,[14] M. Ahmad,[15] J. G. Bian,[15] G. M. Chen,[15] H. S. Chen,[15] M. Chen,[15] T. Cheng,[15] R. Du,[15] C. H. Jiang,[15] R. Plestina,[15,j] F. Romeo,[15] S. M. Shaheen,[15] J. Tao,[15] C. Wang,[15] Z. Wang,[15] H. Zhang,[15] C. Asawatangtrakuldee,[16] Y. Ban,[16] Q. Li,[16] S. Liu,[16] Y. Mao,[16] S. J. Qian,[16] D. Wang,[16] Z. Xu,[16] W. Zou,[16] C. Avila,[17] A. Cabrera,[17] L. F. Chaparro Sierra,[17] C. Florez,[17] J. P. Gomez,[17] B. Gomez Moreno,[17] J. C. Sanabria,[17] N. Godinovic,[18] D. Lelas,[18] I. Puljak,[18] P. M. Ribeiro Cipriano,[18] Z. Antunovic,[19] M. Kovac,[19] V. Brigljevic,[20] K. Kadija,[20] J. Luetic,[20] S. Micanovic,[20] L. Sudic,[20] A. Attikis,[21] G. Mavromanolakis,[21] J. Mousa,[21] C. Nicolaou,[21] F. Ptochos,[21] P. A. Razis,[21] H. Rykaczewski,[21] M. Bodlak,[22] M. Finger,[22,k] M. Finger Jr.,[22,k] M. El Sawy,[23,l,m] E. El-khateeb,[23,n,n] T. Elkafrawy,[23,n] A. Mohamed,[23,o] E. Salama,[23,m,n] B. Calpas,[24] M. Kadastik,[24] M. Murumaa,[24] M. Raidal,[24] A. Tiko,[24] C. Veelken,[24] P. Eerola,[25] J. Pekkanen,[25] M. Voutilainen,[25] J. Härkönen,[26] V. Karimäki,[26] R. Kinnunen,[26] T. Lampén,[26] K. Lassila-Perini,[26] S. Lehti,[26] T. Lindén,[26] P. Luukka,[26] T. Mäenpää,[26] T. Peltola,[26] E. Tuominen,[26] J. Tuominiemi,[26] E. Tuovinen,[26] L. Wendland,[26] J. Talvitie,[27] T. Tuuva,[27] M. Besancon,[28] F. Couderc,[28] M. Dejardin,[28] D. Denegri,[28] B. Fabbro,[28] J. L. Faure,[28] C. Favaro,[28] F. Ferri,[28] S. Ganjour,[28] A. Givernaud,[28] P. Gras,[28] G. Hamel de Monchenault,[28] P. Jarry,[28] E. Locci,[28] M. Machet,[28] J. Malcles,[28] J. Rander,[28] A. Rosowsky,[28] M. Titov,[28] A. Zghiche,[28] I. Antropov,[29] S. Baffioni,[29] F. Beaudette,[29] P. Busson,[29] L. Cadamuro,[29] E. Chapon,[29] C. Charlot,[29]

T. Dahms,[29] O. Davignon,[29] N. Filipovic,[29] A. Florent,[29] R. Granier de Cassagnac,[29] S. Lisniak,[29] L. Mastrolorenzo,[29] P. Miné,[29] I. N. Naranjo,[29] M. Nguyen,[29] C. Ochando,[29] G. Ortona,[29] P. Paganini,[29] P. Pigard,[29] S. Regnard,[29] R. Salerno,[29] J. B. Sauvan,[29] Y. Sirois,[29] T. Strebler,[29] Y. Yilmaz,[29] A. Zabi,[29] J.-L. Agram,[30,p] J. Andrea,[30] A. Aubin,[30] D. Bloch,[30] J.-M. Brom,[30] M. Buttignol,[30] E. C. Chabert,[30] N. Chanon,[30] C. Collard,[30] E. Conte,[30,p] X. Coubez,[30] J.-C. Fontaine,[30,p] D. Gelé,[30] U. Goerlach,[30] C. Goetzmann,[30] A.-C. Le Bihan,[30] J. A. Merlin,[30,c] K. Skovpen,[30] P. Van Hove,[30] S. Gadrat,[31] S. Beauceron,[32] C. Bernet,[32] G. Boudoul,[32] E. Bouvier,[32] C. A. Carrillo Montoya,[32] R. Chierici,[32] D. Contardo,[32] B. Courbon,[32] P. Depasse,[32] H. El Mamouni,[32] J. Fan,[32] J. Fay,[32] S. Gascon,[32] M. Gouzevitch,[32] B. Ille,[32] F. Lagarde,[32] I. B. Laktineh,[32] M. Lethuillier,[32] L. Mirabito,[32] A. L. Pequegnot,[32] S. Perries,[32] J. D. Ruiz Alvarez,[32] D. Sabes,[32] L. Sgandurra,[32] V. Sordini,[32] M. Vander Donckt,[32] P. Verdier,[32] S. Viret,[32] T. Toriashvili,[33,q] Z. Tsamalaidze,[34,k] C. Autermann,[35] S. Beranek,[35] M. Edelhoff,[35] L. Feld,[35] A. Heister,[35] M. K. Kiesel,[35] K. Klein,[35] M. Lipinski,[35] A. Ostapchuk,[35] M. Preuten,[35] F. Raupach,[35] S. Schael,[35] J. F. Schulte,[35] T. Verlage,[35] H. Weber,[35] B. Wittmer,[35] V. Zhukov,[35,g] M. Ata,[36] M. Brodski,[36] E. Dietz-Laursonn,[36] D. Duchardt,[36] M. Endres,[36] M. Erdmann,[36] S. Erdweg,[36] T. Esch,[36] R. Fischer,[36] A. Güth,[36] T. Hebbeker,[36] C. Heidemann,[36] K. Hoepfner,[36] D. Klingebiel,[36] S. Knutzen,[36] P. Kreuzer,[36] M. Merschmeyer,[36] A. Meyer,[36] P. Millet,[36] M. Olschewski,[36] K. Padeken,[36] P. Papacz,[36] T. Pook,[36] M. Radziej,[36] H. Reithler,[36] M. Rieger,[36] F. Scheuch,[36] L. Sonnenschein,[36] D. Teyssier,[36] S. Thüer,[36] V. Cherepanov,[37] Y. Erdogan,[37] G. Flügge,[37] H. Geenen,[37] M. Geisler,[37] F. Hoehle,[37] B. Kargoll,[37] T. Kress,[37] Y. Kuessel,[37] A. Künsken,[37] J. Lingemann,[37,c] A. Nehrkorn,[37] A. Nowack,[37] I. M. Nugent,[37] C. Pistone,[37] O. Pooth,[37] A. Stahl,[37] M. Aldaya Martin,[38] I. Asin,[38] N. Bartosik,[38] O. Behnke,[38] U. Behrens,[38] A. J. Bell,[38] K. Borras,[38] A. Burgmeier,[38] A. Cakir,[38] L. Calligaris,[38] A. Campbell,[38] S. Choudhury,[38] F. Costanza,[38] C. Diez Pardos,[38] G. Dolinska,[38] S. Dooling,[38] T. Dorland,[38] G. Eckerlin,[38] D. Eckstein,[38] T. Eichhorn,[38] G. Flucke,[38] E. Gallo,[38,r] J. Garay Garcia,[38] A. Geiser,[38] A. Gizhko,[38] P. Gunnellini,[38] J. Hauk,[38] M. Hempel,[38,s] H. Jung,[38] A. Kalogeropoulos,[38] O. Karacheban,[38,s] M. Kasemann,[38] P. Katsas,[38] J. Kieseler,[38] C. Kleinwort,[38] I. Korol,[38] W. Lange,[38] J. Leonard,[38] K. Lipka,[38] A. Lobanov,[38] W. Lohmann,[38,s] R. Mankel,[38] I. Marfin,[38,s] I.-A. Melzer-Pellmann,[38] A. B. Meyer,[38] G. Mittag,[38] J. Mnich,[38] A. Mussgiller,[38] S. Naumann-Emme,[38] A. Nayak,[38] E. Ntomari,[38] H. Perrey,[38] D. Pitzl,[38] R. Placakyte,[38] A. Raspereza,[38] B. Roland,[38] M. Ö. Sahin,[38] P. Saxena,[38] T. Schoerner-Sadenius,[38] M. Schröder,[38] C. Seitz,[38] S. Spannagel,[38] K. D. Trippkewitz,[38] R. Walsh,[38] C. Wissing,[38] V. Blobel,[39] M. Centis Vignali,[39] A. R. Draeger,[39] J. Erfle,[39] E. Garutti,[39] K. Goebel,[39] D. Gonzalez,[39] M. Görner,[39] J. Haller,[39] M. Hoffmann,[39] R. S. Höing,[39] A. Junkes,[39] R. Klanner,[39] R. Kogler,[39] T. Lapsien,[39] T. Lenz,[39] I. Marchesini,[39] D. Marconi,[39] M. Meyer,[39] D. Nowatschin,[39] J. Ott,[39] F. Pantaleo,[39,c] T. Peiffer,[39] A. Perieanu,[39] N. Pietsch,[39] J. Poehlsen,[39] D. Rathjens,[39] C. Sander,[39] H. Schettler,[39] P. Schleper,[39] E. Schlieckau,[39] A. Schmidt,[39] J. Schwandt,[39] M. Seidel,[39] V. Sola,[39] H. Stadie,[39] G. Steinbrück,[39] H. Tholen,[39] D. Troendle,[39] E. Usai,[39] L. Vanelderen,[39] A. Vanhoefer,[39] B. Vormwald,[39] M. Akbiyik,[40] C. Barth,[40] C. Baus,[40] J. Berger,[40] C. Böser,[40] E. Butz,[40] T. Chwalek,[40] F. Colombo,[40] W. De Boer,[40] A. Descroix,[40] A. Dierlamm,[40] S. Fink,[40] F. Frensch,[40] M. Giffels,[40] A. Gilbert,[40] F. Hartmann,[40,c] S. M. Heindl,[40] U. Husemann,[40] I. Katkov,[40,g] A. Kornmayer,[40,c] P. Lobelle Pardo,[40] B. Maier,[40] H. Mildner,[40] M. U. Mozer,[40] T. Müller,[40] Th. Müller,[40] M. Plagge,[40] G. Quast,[40] K. Rabbertz,[40] S. Röcker,[40] F. Roscher,[40] H. J. Simonis,[40] F. M. Stober,[40] R. Ulrich,[40] J. Wagner-Kuhr,[40] S. Wayand,[40] M. Weber,[40] T. Weiler,[40] C. Wöhrmann,[40] R. Wolf,[40] G. Anagnostou,[41] G. Daskalakis,[41] T. Geralis,[41] V. A. Giakoumopoulou,[41] A. Kyriakis,[41] D. Loukas,[41] A. Psallidas,[41] I. Topsis-Giotis,[41] A. Agapitos,[42] S. Kesisoglou,[42] A. Panagiotou,[42] N. Saoulidou,[42] E. Tziaferi,[42] I. Evangelou,[43] G. Flouris,[43] C. Foudas,[43] P. Kokkas,[43] N. Loukas,[43] N. Manthos,[43] I. Papadopoulos,[43] E. Paradas,[43] J. Strologas,[43] G. Bencze,[44] C. Hajdu,[44] A. Hazi,[44] P. Hidas,[44] D. Horvath,[44,t] F. Sikler,[44] V. Veszpremi,[44] G. Vesztergombi,[44,u] A. J. Zsigmond,[44] N. Beni,[45] S. Czellar,[45] J. Karancsi,[45,v] J. Molnar,[45] Z. Szillasi,[45] M. Bartók,[46,w] A. Makovec,[46] P. Raics,[46] Z. L. Trocsanyi,[46] B. Ujvari,[46] P. Mal,[47] K. Mandal,[47] D. K. Sahoo,[47] N. Sahoo,[47] S. K. Swain,[47] S. Bansal,[48] S. B. Beri,[48] V. Bhatnagar,[48] R. Chawla,[48] R. Gupta,[48] U. Bhawandeep,[48] A. K. Kalsi,[48] A. Kaur,[48] M. Kaur,[48] R. Kumar,[48] A. Mehta,[48] M. Mittal,[48] J. B. Singh,[48] G. Walia,[48] Ashok Kumar,[49] A. Bhardwaj,[49] B. C. Choudhary,[49] R. B. Garg,[49] A. Kumar,[49] S. Malhotra,[49] M. Naimuddin,[49] N. Nishu,[49] K. Ranjan,[49] R. Sharma,[49] V. Sharma,[49] S. Banerjee,[50] S. Bhattacharya,[50] K. Chatterjee,[50] S. Dey,[50] S. Dutta,[50] Sa. Jain,[50] N. Majumdar,[50] A. Modak,[50] K. Mondal,[50] S. Mukherjee,[50] S. Mukhopadhyay,[50] A. Roy,[50] D. Roy,[50] S. Roy Chowdhury,[50] S. Sarkar,[50] M. Sharan,[50] A. Abdulsalam,[51] R. Chudasama,[51] D. Dutta,[51] V. Jha,[51] V. Kumar,[51] A. K. Mohanty,[51,c] L. M. Pant,[51] P. Shukla,[51] A. Topkar,[51] T. Aziz,[52] S. Banerjee,[52] S. Bhowmik,[52,x] R. M. Chatterjee,[52] R. K. Dewanjee,[52] S. Dugad,[52] S. Ganguly,[52] S. Ghosh,[52] M. Guchait,[52] A. Gurtu,[52,y] G. Kole,[52] S. Kumar,[52] B. Mahakud,[52] M. Maity,[52,x] G. Majumder,[52] K. Mazumdar,[52] S. Mitra,[52] G. B. Mohanty,[52]

B. Parida,[52] T. Sarkar,[52,x] K. Sudhakar,[52] N. Sur,[52] B. Sutar,[52] N. Wickramage,[52,z] S. Chauhan,[53] S. Dube,[53] S. Sharma,[53] H. Bakhshiansohi,[54] H. Behnamian,[54] S. M. Etesami,[54,aa] A. Fahim,[54,bb] R. Goldouzian,[54] M. Khakzad,[54] M. Mohammadi Najafabadi,[54] M. Naseri,[54] S. Paktinat Mehdiabadi,[54] F. Rezaei Hosseinabadi,[54] B. Safarzadeh,[54,cc] M. Zeinali,[54] M. Felcini,[55] M. Grunewald,[55] M. Abbrescia,[56a,56b] C. Calabria,[56a,56b] C. Caputo,[56a,56b] A. Colaleo,[56a] D. Creanza,[56a,56c] L. Cristella,[56a,56b] N. De Filippis,[56a,56c] M. De Palma,[56a,56b] L. Fiore,[56a] G. Iaselli,[56a,56c] G. Maggi,[56a,56c] M. Maggi,[56a] G. Miniello,[56a,56b] S. My,[56a,56c] S. Nuzzo,[56a,56b] A. Pompili,[56a,56b] G. Pugliese,[56a,56c] R. Radogna,[56a,56b] A. Ranieri,[56a] G. Selvaggi,[56a,56b] L. Silvestris,[56a,c] R. Venditti,[56a,56b] P. Verwilligen,[56a] G. Abbiendi,[57a] C. Battilana,[57a,c] A. C. Benvenuti,[57a] D. Bonacorsi,[57a,57b] S. Braibant-Giacomelli,[57a,57b] L. Brigliadori,[57a,57b] R. Campanini,[57a,57b] P. Capiluppi,[57a,57b] A. Castro,[57a,57b] F. R. Cavallo,[57a] S. S. Chhibra,[57a,57b] G. Codispoti,[57a,57b] M. Cuffiani,[57a,57b] G. M. Dallavalle,[57a] F. Fabbri,[57a] A. Fanfani,[57a,57b] D. Fasanella,[57a,57b] P. Giacomelli,[57a] C. Grandi,[57a] L. Guiducci,[57a,57b] S. Marcellini,[57a] G. Masetti,[57a] A. Montanari,[57a] F. L. Navarria,[57a,57b] A. Perrotta,[57a] A. M. Rossi,[57a,57b] T. Rovelli,[57a,57b] G. P. Siroli,[57a,57b] N. Tosi,[57a,57b] R. Travaglini,[57a,57b] G. Cappello,[58a] M. Chiorboli,[58a,58b] S. Costa,[58a,58b] F. Giordano,[58a,58b] R. Potenza,[58a,58b] A. Tricomi,[58a,58b] C. Tuve,[58a,58b] G. Barbagli,[59a] V. Ciulli,[59a,59b] C. Civinini,[59a] R. D'Alessandro,[59a,59b] E. Focardi,[59a,59b] S. Gonzi,[59a,59b] V. Gori,[59a,59b] P. Lenzi,[59a,59b] M. Meschini,[59a] S. Paoletti,[59a] G. Sguazzoni,[59a] A. Tropiano,[59a,59b] L. Viliani,[59a,59b] L. Benussi,[60] S. Bianco,[60] F. Fabbri,[60] D. Piccolo,[60] F. Primavera,[60] V. Calvelli,[61a,61b] F. Ferro,[61a] M. Lo Vetere,[61a,61b] M. R. Monge,[61a,61b] E. Robutti,[61a] S. Tosi,[61a,61b] L. Brianza,[62a] M. E. Dinardo,[62a,62b] S. Fiorendi,[62a,62b] S. Gennai,[62a] R. Gerosa,[62a,62b] A. Ghezzi,[62a,62b] P. Govoni,[62a,62b] S. Malvezzi,[62a] R. A. Manzoni,[62a,62b] B. Marzocchi,[62a,62b,c] D. Menasce,[62a] L. Moroni,[62a] M. Paganoni,[62a,62b] D. Pedrini,[62a] S. Ragazzi,[62a,62b] N. Redaelli,[62a] T. Tabarelli de Fatis,[62a,62b] S. Buontempo,[63a] N. Cavallo,[63a,63c] S. Di Guida,[63a,63d,c] M. Esposito,[63a,63b] F. Fabozzi,[63a,63c] A. O. M. Iorio,[63a,63b] G. Lanza,[63a] L. Lista,[63a] S. Meola,[63a,63d,c] M. Merola,[63a] P. Paolucci,[63a,c] C. Sciacca,[63a,63b] F. Thyssen,[63a] P. Azzi,[64a,c] N. Bacchetta,[64a] L. Benato,[64a,64b] D. Bisello,[64a,64b] A. Boletti,[64a,64b] R. Carlin,[64a,64b] P. Checchia,[64a] M. Dall'Osso,[64a,64b,c] T. Dorigo,[64a] F. Gasparini,[64a,64b] U. Gasparini,[64a,64b] A. Gozzelino,[64a] K. Kanishchev,[64a,64c] S. Lacaprara,[64a] M. Margoni,[64a,64b] A. T. Meneguzzo,[64a,64b] J. Pazzini,[64a,64b] M. Pegoraro,[64a] N. Pozzobon,[64a,64b] P. Ronchese,[64a,64b] M. Sgaravatto,[64a] F. Simonetto,[64a,64b] E. Torassa,[64a] M. Tosi,[64a,64b] S. Vanini,[64a,64b] M. Zanetti,[64a] P. Zotto,[64a,64b] A. Zucchetta,[64a,64b,c] G. Zumerle,[64a,64b] A. Braghieri,[65a] A. Magnani,[65a] P. Montagna,[65a,65b] S. P. Ratti,[65a,65b] V. Re,[65a] C. Riccardi,[65a,65b] P. Salvini,[65a] I. Vai,[65a] P. Vitulo,[65a,65b] L. Alunni Solestizi,[66a,66b] M. Biasini,[66a,66b] G. M. Bilei,[66a] D. Ciangottini,[66a,66b,c] L. Fanò,[66a,66b] P. Lariccia,[66a,66b] G. Mantovani,[66a,66b] M. Menichelli,[66a] A. Saha,[66a] A. Santocchia,[66a,66b] A. Spiezia,[66a,66b] K. Androsov,[67a,dd] P. Azzurri,[67a] G. Bagliesi,[67a] J. Bernardini,[67a] T. Boccali,[67a] G. Broccolo,[67a,67c] R. Castaldi,[67a] M. A. Ciocci,[67a,dd] R. Dell'Orso,[67a] S. Donato,[67a,67c,c] G. Fedi,[67a] L. Foà,[67a,67c,a] A. Giassi,[67a] M. T. Grippo,[67a,dd] F. Ligabue,[67a,67c] T. Lomtadze,[67a] L. Martini,[67a,67b] A. Messineo,[67a,67b] F. Palla,[67a] A. Rizzi,[67a,67b] A. Savoy-Navarro,[67a,ee] A. T. Serban,[67a] P. Spagnolo,[67a] P. Squillacioti,[67a,dd] R. Tenchini,[67a] G. Tonelli,[67a,67b] A. Venturi,[67a] P. G. Verdini,[67a] L. Barone,[68a,68b] F. Cavallari,[68a] G. D'imperio,[68a,68b,c] D. Del Re,[68a,68b] M. Diemoz,[68a] S. Gelli,[68a,68b] C. Jorda,[68a] E. Longo,[68a,68b] F. Margaroli,[68a,68b] P. Meridiani,[68a] G. Organtini,[68a,68b] R. Paramatti,[68a] F. Preiato,[68a,68b] S. Rahatlou,[68a,68b] C. Rovelli,[68a] F. Santanastasio,[68a,68b] P. Traczyk,[68a,68b,c] N. Amapane,[69a,69b] R. Arcidiacono,[69a,69c,c] S. Argiro,[69a,69b] M. Arneodo,[69a,69c] R. Bellan,[69a,69b] C. Biino,[69a] N. Cartiglia,[69a] M. Costa,[69a,69b] R. Covarelli,[69a,69b] P. De Remigis,[69a] A. Degano,[69a,69b] G. Dellacasa,[69a] N. Demaria,[69a] L. Finco,[69a,69b,c] C. Mariotti,[69a] S. Maselli,[69a] E. Migliore,[69a,69b] V. Monaco,[69a,69b] E. Monteil,[69a,69b] M. Musich,[69a] M. M. Obertino,[69a,69b] L. Pacher,[69a,69b] N. Pastrone,[69a] M. Pelliccioni,[69a] G. L. Pinna Angioni,[69a,69b] F. Ravera,[69a,69b] A. Romero,[69a,69b] M. Ruspa,[69a,69c] R. Sacchi,[69a,69b] A. Solano,[69a,69b] A. Staiano,[69a] S. Belforte,[70a] V. Candelise,[70a,70b,c] M. Casarsa,[70a] F. Cossutti,[70a] G. Della Ricca,[70a,70b] B. Gobbo,[70a] C. La Licata,[70a,70b] M. Marone,[70a,70b] A. Schizzi,[70a,70b] A. Zanetti,[70a] A. Kropivnitskaya,[71] S. K. Nam,[71] D. H. Kim,[72] G. N. Kim,[72] M. S. Kim,[72] D. J. Kong,[72] S. Lee,[72] Y. D. Oh,[72] A. Sakharov,[72] D. C. Son,[72] J. A. Brochero Cifuentes,[73] H. Kim,[73] T. J. Kim,[73] M. S. Ryu,[73] S. Song,[74] S. Choi,[75] Y. Go,[75] D. Gyun,[75] B. Hong,[75] M. Jo,[75] H. Kim,[75] Y. Kim,[75] B. Lee,[75] K. Lee,[75] K. S. Lee,[75] S. Lee,[75] S. K. Park,[75] Y. Roh,[75] H. D. Yoo,[76] M. Choi,[77] H. Kim,[77] J. H. Kim,[77] J. S. H. Lee,[77] I. C. Park,[77] G. Ryu,[77] Y. Choi,[78] J. Goh,[78] D. Kim,[78] E. Kwon,[78] J. Lee,[78] I. Yu,[78] A. Juodagalvis,[79] J. Vaitkus,[79] I. Ahmed,[80] Z. A. Ibrahim,[80] J. R. Komaragiri,[80] M. A. B. Md Ali,[80,ff] F. Mohamad Idris,[80,gg] W. A. T. Wan Abdullah,[80] M. N. Yusli,[80] E. Casimiro Linares,[81] H. Castilla-Valdez,[81] E. De La Cruz-Burelo,[81] I. Heredia-de La Cruz,[81,hh] A. Hernandez-Almada,[81] R. Lopez-Fernandez,[81] A. Sanchez-Hernandez,[81] S. Carrillo Moreno,[82] F. Vazquez Valencia,[82] I. Pedraza,[83] H. A. Salazar Ibarguen,[83] A. Morelos Pineda,[84] D. Krofcheck,[85] P. H. Butler,[86] A. Ahmad,[87] M. Ahmad,[87] Q. Hassan,[87] H. R. Hoorani,[87] W. A. Khan,[87] T. Khurshid,[87] M. Shoaib,[87] H. Bialkowska,[88]

M. Bluj,[88] B. Boimska,[88] T. Frueboes,[88] M. Górski,[88] M. Kazana,[88] K. Nawrocki,[88] K. Romanowska-Rybinska,[88] M. Szleper,[88] P. Zalewski,[88] G. Brona,[89] K. Bunkowski,[89] A. Byszuk,[89,ii] K. Doroba,[89] A. Kalinowski,[89] M. Konecki,[89] J. Krolikowski,[89] M. Misiura,[89] M. Olszewski,[89] M. Walczak,[89] P. Bargassa,[90] C. Beirão Da Cruz E Silva,[90] A. Di Francesco,[90] P. Faccioli,[90] P. G. Ferreira Parracho,[90] M. Gallinaro,[90] N. Leonardo,[90] L. Lloret Iglesias,[90] F. Nguyen,[90] J. Rodrigues Antunes,[90] J. Seixas,[90] O. Toldaiev,[90] D. Vadruccio,[90] J. Varela,[90] P. Vischia,[90] S. Afanasiev,[91] P. Bunin,[91] M. Gavrilenko,[91] I. Golutvin,[91] I. Gorbunov,[91] A. Kamenev,[91] V. Karjavin,[91] V. Konoplyanikov,[91] A. Lanev,[91] A. Malakhov,[91] V. Matveev,[91,jj] P. Moisenz,[91] V. Palichik,[91] V. Perelygin,[91] S. Shmatov,[91] S. Shulha,[91] N. Skatchkov,[91] V. Smirnov,[91] A. Zarubin,[91] V. Golovtsov,[92] Y. Ivanov,[92] V. Kim,[92,kk] E. Kuznetsova,[92] P. Levchenko,[92] V. Murzin,[92] V. Oreshkin,[92] I. Smirnov,[92] V. Sulimov,[92] L. Uvarov,[92] S. Vavilov,[92] A. Vorobyev,[92] Yu. Andreev,[93] A. Dermenev,[93] S. Gninenko,[93] N. Golubev,[93] A. Karneyeu,[93] M. Kirsanov,[93] N. Krasnikov,[93] A. Pashenkov,[93] D. Tlisov,[93] A. Toropin,[93] V. Epshteyn,[94] V. Gavrilov,[94] N. Lychkovskaya,[94] V. Popov,[94] I. Pozdnyakov,[94] G. Safronov,[94] A. Spiridonov,[94] E. Vlasov,[94] A. Zhokin,[94] A. Bylinkin,[95] V. Andreev,[96] M. Azarkin,[96,ll] I. Dremin,[96,ll] M. Kirakosyan,[96] A. Leonidov,[96,ll] G. Mesyats,[96] S. V. Rusakov,[96] A. Vinogradov,[96] A. Baskakov,[97] A. Belyaev,[97] E. Boos,[97] V. Bunichev,[97] M. Dubinin,[97,mm] L. Dudko,[97] A. Ershov,[97] A. Gribushin,[97] V. Klyukhin,[97] O. Kodolova,[97] I. Lokhtin,[97] I. Myagkov,[97] S. Obraztsov,[97] V. Savrin,[97] A. Snigirev,[97] I. Azhgirey,[98] I. Bayshev,[98] S. Bitioukov,[98] V. Kachanov,[98] A. Kalinin,[98] D. Konstantinov,[98] V. Krychkine,[98] V. Petrov,[98] R. Ryutin,[98] A. Sobol,[98] L. Tourtchanovitch,[98] S. Troshin,[98] N. Tyurin,[98] A. Uzunian,[98] A. Volkov,[98] P. Adzic,[99,nn] M. Ekmedzic,[99] J. Milosevic,[99] V. Rekovic,[99] J. Alcaraz Maestre,[100] E. Calvo,[100] M. Cerrada,[100] M. Chamizo Llatas,[100] N. Colino,[100] B. De La Cruz,[100] A. Delgado Peris,[100] D. Domínguez Vázquez,[100] A. Escalante Del Valle,[100] C. Fernandez Bedoya,[100] J. P. Fernández Ramos,[100] J. Flix,[100] M. C. Fouz,[100] P. Garcia-Abia,[100] O. Gonzalez Lopez,[100] S. Goy Lopez,[100] J. M. Hernandez,[100] M. I. Josa,[100] E. Navarro De Martino,[100] A. Pérez-Calero Yzquierdo,[100] J. Puerta Pelayo,[100] A. Quintario Olmeda,[100] I. Redondo,[100] L. Romero,[100] M. S. Soares,[100] C. Albajar,[101] J. F. de Trocóniz,[101] M. Missiroli,[101] D. Moran,[101] J. Cuevas,[102] J. Fernandez Menendez,[102] S. Folgueras,[102] I. Gonzalez Caballero,[102] E. Palencia Cortezon,[102] J. M. Vizan Garcia,[102] I. J. Cabrillo,[103] A. Calderon,[103] J. R. Castiñeiras De Saa,[103] P. De Castro Manzano,[103] J. Duarte Campderros,[103] M. Fernandez,[103] J. Garcia-Ferrero,[103] G. Gomez,[103] A. Lopez Virto,[103] J. Marco,[103] R. Marco,[103] C. Martinez Rivero,[103] F. Matorras,[103] F. J. Munoz Sanchez,[103] J. Piedra Gomez,[103] T. Rodrigo,[103] A. Y. Rodríguez-Marrero,[103] A. Ruiz-Jimeno,[103] L. Scodellaro,[103] I. Vila,[103] R. Vilar Cortabitarte,[103] D. Abbaneo,[104] E. Auffray,[104] G. Auzinger,[104] M. Bachtis,[104] P. Baillon,[104] A. H. Ball,[104] D. Barney,[104] A. Benaglia,[104] J. Bendavid,[104] L. Benhabib,[104] J. F. Benitez,[104] G. M. Berruti,[104] P. Bloch,[104] A. Bocci,[104] A. Bonato,[104] C. Botta,[104] H. Breuker,[104] T. Camporesi,[104] G. Cerminara,[104] S. Colafranceschi,[104,oo] M. D'Alfonso,[104] D. d'Enterria,[104] A. Dabrowski,[104] V. Daponte,[104] A. David,[104] M. De Gruttola,[104] F. De Guio,[104] A. De Roeck,[104] S. De Visscher,[104] E. Di Marco,[104] M. Dobson,[104] M. Dordevic,[104] B. Dorney,[104] T. du Pree,[104] M. Dünser,[104] N. Dupont,[104] A. Elliott-Peisert,[104] G. Franzoni,[104] W. Funk,[104] D. Gigi,[104] K. Gill,[104] D. Giordano,[104] M. Girone,[104] F. Glege,[104] R. Guida,[104] S. Gundacker,[104] M. Guthoff,[104] J. Hammer,[104] P. Harris,[104] J. Hegeman,[104] V. Innocente,[104] P. Janot,[104] H. Kirschenmann,[104] M. J. Kortelainen,[104] K. Kousouris,[104] K. Krajczar,[104] P. Lecoq,[104] C. Lourenço,[104] M. T. Lucchini,[104] N. Magini,[104] L. Malgeri,[104] M. Mannelli,[104] A. Martelli,[104] L. Masetti,[104] F. Meijers,[104] S. Mersi,[104] E. Meschi,[104] F. Moortgat,[104] S. Morovic,[104] M. Mulders,[104] M. V. Nemallapudi,[104] H. Neugebauer,[104] S. Orfanelli,[104,pp] L. Orsini,[104] L. Pape,[104] E. Perez,[104] M. Peruzzi,[104] A. Petrilli,[104] G. Petrucciani,[104] A. Pfeiffer,[104] D. Piparo,[104] A. Racz,[104] G. Rolandi,[104,qq] M. Rovere,[104] M. Ruan,[104] H. Sakulin,[104] C. Schäfer,[104] C. Schwick,[104] A. Sharma,[104] P. Silva,[104] M. Simon,[104] P. Sphicas,[104,rr] D. Spiga,[104] J. Steggemann,[104] B. Stieger,[104] M. Stoye,[104] Y. Takahashi,[104] D. Treille,[104] A. Triossi,[104] A. Tsirou,[104] G. I. Veres,[104,u] N. Wardle,[104] H. K. Wöhri,[104] A. Zagozdzinska,[104,ii] W. D. Zeuner,[104] W. Bertl,[105] K. Deiters,[105] W. Erdmann,[105] R. Horisberger,[105] Q. Ingram,[105] H. C. Kaestli,[105] D. Kotlinski,[105] U. Langenegger,[105] D. Renker,[105] T. Rohe,[105] F. Bachmair,[106] L. Bäni,[106] L. Bianchini,[106] M. A. Buchmann,[106] B. Casal,[106] G. Dissertori,[106] M. Dittmar,[106] M. Donegà,[106] P. Eller,[106] C. Grab,[106] C. Heidegger,[106] D. Hits,[106] J. Hoss,[106] G. Kasieczka,[106] W. Lustermann,[106] B. Mangano,[106] M. Marionneau,[106] P. Martinez Ruiz del Arbol,[106] M. Masciovecchio,[106] D. Meister,[106] F. Micheli,[106] P. Musella,[106] F. Nessi-Tedaldi,[106] F. Pandolfi,[106] J. Pata,[106] F. Pauss,[106] L. Perrozzi,[106] M. Quittnat,[106] M. Rossini,[106] A. Starodumov,[106,ss] M. Takahashi,[106] V. R. Tavolaro,[106] K. Theofilatos,[106] R. Wallny,[106] T. K. Aarrestad,[107] C. Amsler,[107,tt] L. Caminada,[107] M. F. Canelli,[107] V. Chiochia,[107] A. De Cosa,[107] C. Galloni,[107] A. Hinzmann,[107] T. Hreus,[107] B. Kilminster,[107] C. Lange,[107] J. Ngadiuba,[107] D. Pinna,[107] P. Robmann,[107] F. J. Ronga,[107] D. Salerno,[107] Y. Yang,[107] M. Cardaci,[108] K. H. Chen,[108] T. H. Doan,[108] Sh. Jain,[108] R. Khurana,[108]

M. Konyushikhin,[108] C. M. Kuo,[108] W. Lin,[108] Y. J. Lu,[108] S. S. Yu,[108] Arun Kumar,[109] R. Bartek,[109] P. Chang,[109] Y. H. Chang,[109] Y. W. Chang,[109] Y. Chao,[109] K. F. Chen,[109] P. H. Chen,[109] C. Dietz,[109] F. Fiori,[109] U. Grundler,[109] W.-S. Hou,[109] Y. Hsiung,[109] Y. F. Liu,[109] R.-S. Lu,[109] M. Miñano Moya,[109] E. Petrakou,[109] J. f. Tsai,[109] Y. M. Tzeng,[109] B. Asavapibhop,[110] K. Kovitanggoon,[110] G. Singh,[110] N. Srimanobhas,[110] N. Suwonjandee,[110] A. Adiguzel,[111] M. N. Bakirci,[111,uu] Z. S. Demiroglu,[111] C. Dozen,[111] I. Dumanoglu,[111] E. Eskut,[111] S. Girgis,[111] G. Gokbulut,[111] Y. Guler,[111] E. Gurpinar,[111] I. Hos,[111] E. E. Kangal,[111,vv] G. Onengut,[111,ww] K. Ozdemir,[111,xx] A. Polatoz,[111] D. Sunar Cerci,[111,yy] H. Topakli,[111,uu] M. Vergili,[111] C. Zorbilmez,[111] I. V. Akin,[112] B. Bilin,[112] S. Bilmis,[112] B. Isildak,[112,zz] G. Karapinar,[112,aaa] M. Yalvac,[112] M. Zeyrek,[112] E. A. Albayrak,[113,bbb] E. Gülmez,[113] M. Kaya,[113,ccc] O. Kaya,[113,ddd] T. Yetkin,[113,eee] K. Cankocak,[114] S. Sen,[114,fff] F. I. Vardarlı,[114] B. Grynyov,[115] L. Levchuk,[116] P. Sorokin,[116] R. Aggleton,[117] F. Ball,[117] L. Beck,[117] J. J. Brooke,[117] E. Clement,[117] D. Cussans,[117] H. Flacher,[117] J. Goldstein,[117] M. Grimes,[117] G. P. Heath,[117] H. F. Heath,[117] J. Jacob,[117] L. Kreczko,[117] C. Lucas,[117] Z. Meng,[117] D. M. Newbold,[117,ggg] S. Paramesvaran,[117] A. Poll,[117] T. Sakuma,[117] S. Seif El Nasr-storey,[117] S. Senkin,[117] D. Smith,[117] V. J. Smith,[117] K. W. Bell,[118] A. Belyaev,[118,hhh] C. Brew,[118] R. M. Brown,[118] D. Cieri,[118] D. J. A. Cockerill,[118] J. A. Coughlan,[118] K. Harder,[118] S. Harper,[118] E. Olaiya,[118] D. Petyt,[118] C. H. Shepherd-Themistocleous,[118] A. Thea,[118] L. Thomas,[118] I. R. Tomalin,[118] T. Williams,[118] W. J. Womersley,[118] S. D. Worm,[118] M. Baber,[119] R. Bainbridge,[119] O. Buchmuller,[119] A. Bundock,[119] D. Burton,[119] S. Casasso,[119] M. Citron,[119] D. Colling,[119] L. Corpe,[119] N. Cripps,[119] P. Dauncey,[119] G. Davies,[119] A. De Wit,[119] M. Della Negra,[119] P. Dunne,[119] A. Elwood,[119] W. Ferguson,[119] J. Fulcher,[119] D. Futyan,[119] G. Hall,[119] G. Iles,[119] M. Kenzie,[119] R. Lane,[119] R. Lucas,[119,ggg] L. Lyons,[119] A.-M. Magnan,[119] S. Malik,[119] J. Nash,[119] A. Nikitenko,[119,ss] J. Pela,[119] M. Pesaresi,[119] K. Petridis,[119] D. M. Raymond,[119] A. Richards,[119] A. Rose,[119] C. Seez,[119] A. Tapper,[119] K. Uchida,[119] M. Vazquez Acosta,[119,iii] T. Virdee,[119] S. C. Zenz,[119] J. E. Cole,[120] P. R. Hobson,[120] A. Khan,[120] P. Kyberd,[120] D. Leggat,[120] D. Leslie,[120] I. D. Reid,[120] P. Symonds,[120] L. Teodorescu,[120] M. Turner,[120] A. Borzou,[121] K. Call,[121] J. Dittmann,[121] K. Hatakeyama,[121] A. Kasmi,[121] H. Liu,[121] N. Pastika,[121] O. Charaf,[122] S. I. Cooper,[122] C. Henderson,[122] P. Rumerio,[122] A. Avetisyan,[123] T. Bose,[123] C. Fantasia,[123] D. Gastler,[123] P. Lawson,[123] D. Rankin,[123] C. Richardson,[123] J. Rohlf,[123] J. St. John,[123] L. Sulak,[123] D. Zou,[123] J. Alimena,[124] E. Berry,[124] S. Bhattacharya,[124] D. Cutts,[124] N. Dhingra,[124] A. Ferapontov,[124] A. Garabedian,[124] J. Hakala,[124] U. Heintz,[124] G. Kukartsev,[124] E. Laird,[124] G. Landsberg,[124] M. Luk,[124] Z. Mao,[124] M. Narain,[124] S. Piperov,[124] S. Sagir,[124] T. Sinthuprasith,[124] T. Speer,[124] R. Syarif,[124] R. Breedon,[125] G. Breto,[125] M. Calderon De La Barca Sanchez,[125] S. Chauhan,[125] M. Chertok,[125] J. Conway,[125] R. Conway,[125] P. T. Cox,[125] R. Erbacher,[125] M. Gardner,[125] W. Ko,[125] R. Lander,[125] M. Mulhearn,[125] D. Pellett,[125] J. Pilot,[125] F. Ricci-Tam,[125] S. Shalhout,[125] J. Smith,[125] M. Squires,[125] D. Stolp,[125] M. Tripathi,[125] S. Wilbur,[125] R. Yohay,[125] R. Cousins,[126] P. Everaerts,[126] C. Farrell,[126] J. Hauser,[126] M. Ignatenko,[126] D. Saltzberg,[126] E. Takasugi,[126] V. Valuev,[126] M. Weber,[126] K. Burt,[127] R. Clare,[127] J. Ellison,[127] J. W. Gary,[127] G. Hanson,[127] J. Heilman,[127] M. Ivova PANEVA,[127] P. Jandir,[127] E. Kennedy,[127] F. Lacroix,[127] O. R. Long,[127] A. Luthra,[127] M. Malberti,[127] M. Olmedo Negrete,[127] A. Shrinivas,[127] H. Wei,[127] S. Wimpenny,[127] B. R. Yates,[127] J. G. Branson,[128] G. B. Cerati,[128] S. Cittolin,[128] R. T. D'Agnolo,[128] A. Holzner,[128] R. Kelley,[128] D. Klein,[128] J. Letts,[128] I. Macneill,[128] D. Olivito,[128] S. Padhi,[128] M. Pieri,[128] M. Sani,[128] V. Sharma,[128] S. Simon,[128] M. Tadel,[128] A. Vartak,[128] S. Wasserbaech,[128,jjj] C. Welke,[128] F. Würthwein,[128] A. Yagil,[128] G. Zevi Della Porta,[128] D. Barge,[129] J. Bradmiller-Feld,[129] C. Campagnari,[129] A. Dishaw,[129] V. Dutta,[129] K. Flowers,[129] M. Franco Sevilla,[129] P. Geffert,[129] C. George,[129] F. Golf,[129] L. Gouskos,[129] J. Gran,[129] J. Incandela,[129] C. Justus,[129] N. Mccoll,[129] S. D. Mullin,[129] J. Richman,[129] D. Stuart,[129] I. Suarez,[129] W. To,[129] C. West,[129] J. Yoo,[129] D. Anderson,[130] A. Apresyan,[130] A. Bornheim,[130] J. Bunn,[130] Y. Chen,[130] J. Duarte,[130] A. Mott,[130] H. B. Newman,[130] C. Pena,[130] M. Pierini,[130] M. Spiropulu,[130] J. R. Vlimant,[130] S. Xie,[130] R. Y. Zhu,[130] M. B. Andrews,[131] V. Azzolini,[131] A. Calamba,[131] B. Carlson,[131] T. Ferguson,[131] M. Paulini,[131] J. Russ,[131] M. Sun,[131] H. Vogel,[131] I. Vorobiev,[131] J. P. Cumalat,[132] W. T. Ford,[132] A. Gaz,[132] F. Jensen,[132] A. Johnson,[132] M. Krohn,[132] T. Mulholland,[132] U. Nauenberg,[132] K. Stenson,[132] S. R. Wagner,[132] J. Alexander,[133] A. Chatterjee,[133] J. Chaves,[133] J. Chu,[133] S. Dittmer,[133] N. Eggert,[133] N. Mirman,[133] G. Nicolas Kaufman,[133] J. R. Patterson,[133] A. Rinkevicius,[133] A. Ryd,[133] L. Skinnari,[133] L. Soffi,[133] W. Sun,[133] S. M. Tan,[133] W. D. Teo,[133] J. Thom,[133] J. Thompson,[133] J. Tucker,[133] Y. Weng,[133] P. Wittich,[133] S. Abdullin,[134] M. Albrow,[134] J. Anderson,[134] G. Apollinari,[134] L. A. T. Bauerdick,[134] A. Beretvas,[134] J. Berryhill,[134] P. C. Bhat,[134] G. Bolla,[134] K. Burkett,[134] J. N. Butler,[134] H. W. K. Cheung,[134] F. Chlebana,[134] S. Cihangir,[134] V. D. Elvira,[134] I. Fisk,[134] J. Freeman,[134] E. Gottschalk,[134] L. Gray,[134] D. Green,[134] S. Grünendahl,[134] O. Gutsche,[134] J. Hanlon,[134] D. Hare,[134] R. M. Harris,[134] J. Hirschauer,[134] Z. Hu,[134] S. Jindariani,[134] M. Johnson,[134] U. Joshi,[134] A. W. Jung,[134] B. Klima,[134] B. Kreis,[134] S. Kwan,[134,a]

S. Lammel,[134] J. Linacre,[134] D. Lincoln,[134] R. Lipton,[134] T. Liu,[134] R. Lopes De Sá,[134] J. Lykken,[134] K. Maeshima,[134] J. M. Marraffino,[134] V. I. Martinez Outschoorn,[134] S. Maruyama,[134] D. Mason,[134] P. McBride,[134] P. Merkel,[134] K. Mishra,[134] S. Mrenna,[134] S. Nahn,[134] C. Newman-Holmes,[134] V. O'Dell,[134] K. Pedro,[134] O. Prokofyev,[134] G. Rakness,[134] E. Sexton-Kennedy,[134] A. Soha,[134] W. J. Spalding,[134] L. Spiegel,[134] L. Taylor,[134] S. Tkaczyk,[134] N. V. Tran,[134] L. Uplegger,[134] E. W. Vaandering,[134] C. Vernieri,[134] M. Verzocchi,[134] R. Vidal,[134] H. A. Weber,[134] A. Whitbeck,[134] F. Yang,[134] D. Acosta,[135] P. Avery,[135] P. Bortignon,[135] D. Bourilkov,[135] A. Carnes,[135] M. Carver,[135] D. Curry,[135] S. Das,[135] G. P. Di Giovanni,[135] R. D. Field,[135] I. K. Furic,[135] J. Hugon,[135] J. Konigsberg,[135] A. Korytov,[135] J. F. Low,[135] P. Ma,[135] K. Matchev,[135] H. Mei,[135] P. Milenovic,[135,kkk] G. Mitselmakher,[135] D. Rank,[135] R. Rossin,[135] L. Shchutska,[135] M. Snowball,[135] D. Sperka,[135] N. Terentyev,[135] J. Wang,[135] S. Wang,[135] J. Yelton,[135] S. Hewamanage,[136] S. Linn,[136] P. Markowitz,[136] G. Martinez,[136] J. L. Rodriguez,[136] A. Ackert,[137] J. R. Adams,[137] T. Adams,[137] A. Askew,[137] J. Bochenek,[137] B. Diamond,[137] J. Haas,[137] S. Hagopian,[137] V. Hagopian,[137] K. F. Johnson,[137] A. Khatiwada,[137] H. Prosper,[137] V. Veeraraghavan,[137] M. Weinberg,[137] M. M. Baarmand,[138] V. Bhopatkar,[138] M. Hohlmann,[138] H. Kalakhety,[138] D. Noonan,[138] T. Roy,[138] F. Yumiceva,[138] M. R. Adams,[139] L. Apanasevich,[139] D. Berry,[139] R. R. Betts,[139] I. Bucinskaite,[139] R. Cavanaugh,[139] O. Evdokimov,[139] L. Gauthier,[139] C. E. Gerber,[139] D. J. Hofman,[139] P. Kurt,[139] C. O'Brien,[139] I. D. Sandoval Gonzalez,[139] C. Silkworth,[139] P. Turner,[139] N. Varelas,[139] Z. Wu,[139] M. Zakaria,[139] B. Bilki,[140,lll] W. Clarida,[140] K. Dilsiz,[140] S. Durgut,[140] R. P. Gandrajula,[140] M. Haytmyradov,[140] V. Khristenko,[140] J.-P. Merlo,[140] H. Mermerkaya,[140,mmm] A. Mestvirishvili,[140] A. Moeller,[140] J. Nachtman,[140] H. Ogul,[140] Y. Onel,[140] F. Ozok,[140,bbb] A. Penzo,[140] C. Snyder,[140] P. Tan,[140] E. Tiras,[140] J. Wetzel,[140] K. Yi,[140] I. Anderson,[141] B. A. Barnett,[141] B. Blumenfeld,[141] D. Fehling,[141] L. Feng,[141] A. V. Gritsan,[141] P. Maksimovic,[141] C. Martin,[141] M. Osherson,[141] M. Swartz,[141] M. Xiao,[141] Y. Xin,[141] C. You,[141] P. Baringer,[142] A. Bean,[142] G. Benelli,[142] C. Bruner,[142] R. P. Kenny III,[142] D. Majumder,[142] M. Malek,[142] M. Murray,[142] S. Sanders,[142] R. Stringer,[142] Q. Wang,[142] A. Ivanov,[143] K. Kaadze,[143] S. Khalil,[143] M. Makouski,[143] Y. Maravin,[143] A. Mohammadi,[143] L. K. Saini,[143] N. Skhirtladze,[143] S. Toda,[143] D. Lange,[144] F. Rebassoo,[144] D. Wright,[144] C. Anelli,[145] A. Baden,[145] O. Baron,[145] A. Belloni,[145] B. Calvert,[145] S. C. Eno,[145] C. Ferraioli,[145] J. A. Gomez,[145] N. J. Hadley,[145] S. Jabeen,[145] R. G. Kellogg,[145] T. Kolberg,[145] J. Kunkle,[145] Y. Lu,[145] A. C. Mignerey,[145] Y. H. Shin,[145] A. Skuja,[145] M. B. Tonjes,[145] S. C. Tonwar,[145] A. Apyan,[146] R. Barbieri,[146] A. Baty,[146] K. Bierwagen,[146] S. Brandt,[146] W. Busza,[146] I. A. Cali,[146] Z. Demiragli,[146] L. Di Matteo,[146] G. Gomez Ceballos,[146] M. Goncharov,[146] D. Gulhan,[146] Y. Iiyama,[146] G. M. Innocenti,[146] M. Klute,[146] D. Kovalskyi,[146] Y. S. Lai,[146] Y.-J. Lee,[146] A. Levin,[146] P. D. Luckey,[146] A. C. Marini,[146] C. Mcginn,[146] C. Mironov,[146] X. Niu,[146] C. Paus,[146] D. Ralph,[146] C. Roland,[146] G. Roland,[146] J. Salfeld-Nebgen,[146] G. S. F. Stephans,[146] K. Sumorok,[146] M. Varma,[146] D. Velicanu,[146] J. Veverka,[146] J. Wang,[146] T. W. Wang,[146] B. Wyslouch,[146] M. Yang,[146] V. Zhukova,[146] B. Dahmes,[147] A. Evans,[147] A. Finkel,[147] A. Gude,[147] P. Hansen,[147] S. Kalafut,[147] S. C. Kao,[147] K. Klapoetke,[147] Y. Kubota,[147] Z. Lesko,[147] J. Mans,[147] S. Nourbakhsh,[147] N. Ruckstuhl,[147] R. Rusack,[147] N. Tambe,[147] J. Turkewitz,[147] J. G. Acosta,[148] S. Oliveros,[148] E. Avdeeva,[149] K. Bloom,[149] S. Bose,[149] D. R. Claes,[149] A. Dominguez,[149] C. Fangmeier,[149] R. Gonzalez Suarez,[149] R. Kamalieddin,[149] J. Keller,[149] D. Knowlton,[149] I. Kravchenko,[149] J. Lazo-Flores,[149] F. Meier,[149] J. Monroy,[149] F. Ratnikov,[149] J. E. Siado,[149] G. R. Snow,[149] M. Alyari,[150] J. Dolen,[150] J. George,[150] A. Godshalk,[150] C. Harrington,[150] I. Iashvili,[150] J. Kaisen,[150] A. Kharchilava,[150] A. Kumar,[150] S. Rappoccio,[150] G. Alverson,[151] E. Barberis,[151] D. Baumgartel,[151] M. Chasco,[151] A. Hortiangtham,[151] A. Massironi,[151] D. M. Morse,[151] D. Nash,[151] T. Orimoto,[151] R. Teixeira De Lima,[151] D. Trocino,[151] R.-J. Wang,[151] D. Wood,[151] J. Zhang,[151] K. A. Hahn,[152] A. Kubik,[152] N. Mucia,[152] N. Odell,[152] B. Pollack,[152] A. Pozdnyakov,[152] M. Schmitt,[152] S. Stoynev,[152] K. Sung,[152] M. Trovato,[152] M. Velasco,[152] A. Brinkerhoff,[153] N. Dev,[153] M. Hildreth,[153] C. Jessop,[153] D. J. Karmgard,[153] N. Kellams,[153] K. Lannon,[153] S. Lynch,[153] N. Marinelli,[153] F. Meng,[153] C. Mueller,[153] Y. Musienko,[153,jj] T. Pearson,[153] M. Planer,[153] A. Reinsvold,[153] R. Ruchti,[153] G. Smith,[153] S. Taroni,[153] N. Valls,[153] M. Wayne,[153] M. Wolf,[153] A. Woodard,[153] L. Antonelli,[154] J. Brinson,[154] B. Bylsma,[154] L. S. Durkin,[154] S. Flowers,[154] A. Hart,[154] C. Hill,[154] R. Hughes,[154] W. Ji,[154] K. Kotov,[154] T. Y. Ling,[154] B. Liu,[154] W. Luo,[154] D. Puigh,[154] M. Rodenburg,[154] B. L. Winer,[154] H. W. Wulsin,[154] O. Driga,[155] P. Elmer,[155] J. Hardenbrook,[155] P. Hebda,[155] S. A. Koay,[155] P. Lujan,[155] D. Marlow,[155] T. Medvedeva,[155] M. Mooney,[155] J. Olsen,[155] C. Palmer,[155] P. Piroué,[155] X. Quan,[155] H. Saka,[155] D. Stickland,[155] C. Tully,[155] J. S. Werner,[155] A. Zuranski,[155] S. Malik,[156] V. E. Barnes,[157] D. Benedetti,[157] D. Bortoletto,[157] L. Gutay,[157] M. K. Jha,[157] M. Jones,[157] K. Jung,[157] M. Kress,[157] D. H. Miller,[157] N. Neumeister,[157] B. C. Radburn-Smith,[157] X. Shi,[157] I. Shipsey,[157] D. Silvers,[157] J. Sun,[157] A. Svyatkovskiy,[157] F. Wang,[157] W. Xie,[157] L. Xu,[157] N. Parashar,[158] J. Stupak,[158] A. Adair,[159] B. Akgun,[159] Z. Chen,[159] K. M. Ecklund,[159] F. J. M. Geurts,[159]

M. Guilbaud,[159] W. Li,[159] B. Michlin,[159] M. Northup,[159] B. P. Padley,[159] R. Redjimi,[159] J. Roberts,[159] J. Rorie,[159] Z. Tu,[159] J. Zabel,[159] B. Betchart,[160] A. Bodek,[160] P. de Barbaro,[160] R. Demina,[160] Y. Eshaq,[160] T. Ferbel,[160] M. Galanti,[160] A. Garcia-Bellido,[160] J. Han,[160] A. Harel,[160] O. Hindrichs,[160] A. Khukhunaishvili,[160] G. Petrillo,[160] M. Verzetti,[160] L. Demortier,[161] S. Arora,[162] A. Barker,[162] J. P. Chou,[162] C. Contreras-Campana,[162] E. Contreras-Campana,[162] D. Duggan,[162] D. Ferencek,[162] Y. Gershtein,[162] R. Gray,[162] E. Halkiadakis,[162] D. Hidas,[162] E. Hughes,[162] S. Kaplan,[162] R. Kunnawalkam Elayavalli,[162] A. Lath,[162] K. Nash,[162] S. Panwalkar,[162] M. Park,[162] S. Salur,[162] S. Schnetzer,[162] D. Sheffield,[162] S. Somalwar,[162] R. Stone,[162] S. Thomas,[162] P. Thomassen,[162] M. Walker,[162] M. Foerster,[163] G. Riley,[163] K. Rose,[163] S. Spanier,[163] A. York,[163] O. Bouhali,[164,nnn] A. Castaneda Hernandez,[164,nnn] M. Dalchenko,[164] M. De Mattia,[164] A. Delgado,[164] S. Dildick,[164] R. Eusebi,[164] W. Flanagan,[164] J. Gilmore,[164] T. Kamon,[164,ooo] V. Krutelyov,[164] R. Mueller,[164] I. Osipenkov,[164] Y. Pakhotin,[164] R. Patel,[164] A. Perloff,[164] A. Rose,[164] A. Safonov,[164] A. Tatarinov,[164] K. A. Ulmer,[164,c] N. Akchurin,[165] C. Cowden,[165] J. Damgov,[165] C. Dragoiu,[165] P. R. Dudero,[165] J. Faulkner,[165] S. Kunori,[165] K. Lamichhane,[165] S. W. Lee,[165] T. Libeiro,[165] S. Undleeb,[165] I. Volobouev,[165] E. Appelt,[166] A. G. Delannoy,[166] S. Greene,[166] A. Gurrola,[166] R. Janjam,[166] W. Johns,[166] C. Maguire,[166] Y. Mao,[166] A. Melo,[166] H. Ni,[166] P. Sheldon,[166] B. Snook,[166] S. Tuo,[166] J. Velkovska,[166] Q. Xu,[166] M. W. Arenton,[167] S. Boutle,[167] B. Cox,[167] B. Francis,[167] J. Goodell,[167] R. Hirosky,[167] A. Ledovskoy,[167] H. Li,[167] C. Lin,[167] C. Neu,[167] X. Sun,[167] Y. Wang,[167] E. Wolfe,[167] J. Wood,[167] F. Xia,[167] C. Clarke,[168] R. Harr,[168] P. E. Karchin,[168] C. Kottachchi Kankanamge Don,[168] P. Lamichhane,[168] J. Sturdy,[168] D. A. Belknap,[169] D. Carlsmith,[169] M. Cepeda,[169] A. Christian,[169] S. Dasu,[169] L. Dodd,[169] S. Duric,[169] E. Friis,[169] B. Gomber,[169] R. Hall-Wilton,[169] M. Herndon,[169] A. Hervé,[169] P. Klabbers,[169] A. Lanaro,[169] A. Levine,[169] K. Long,[169] R. Loveless,[169] A. Mohapatra,[169] I. Ojalvo,[169] T. Perry,[169] G. A. Pierro,[169] G. Polese,[169] T. Ruggles,[169] T. Sarangi,[169] A. Savin,[169] A. Sharma,[169] N. Smith,[169] W. H. Smith,[169] D. Taylor,[169] and N. Woods[169]

(CMS Collaboration)

[1]*Yerevan Physics Institute, Yerevan, Armenia*
[2]*Institut für Hochenergiephysik der OeAW, Wien, Austria*
[3]*National Centre for Particle and High Energy Physics, Minsk, Belarus*
[4]*Universiteit Antwerpen, Antwerpen, Belgium*
[5]*Vrije Universiteit Brussel, Brussel, Belgium*
[6]*Université Libre de Bruxelles, Bruxelles, Belgium*
[7]*Ghent University, Ghent, Belgium*
[8]*Université Catholique de Louvain, Louvain-la-Neuve, Belgium*
[9]*Université de Mons, Mons, Belgium*
[10]*Centro Brasileiro de Pesquisas Fisicas, Rio de Janeiro, Brazil*
[11]*Universidade do Estado do Rio de Janeiro, Rio de Janeiro, Brazil*
[12a]*Universidade Estadual Paulista, São Paulo, Brazil*
[12b]*Universidade Federal do ABC, São Paulo, Brazil*
[13]*Institute for Nuclear Research and Nuclear Energy, Sofia, Bulgaria*
[14]*University of Sofia, Sofia, Bulgaria*
[15]*Institute of High Energy Physics, Beijing, China*
[16]*State Key Laboratory of Nuclear Physics and Technology, Peking University, Beijing, China*
[17]*Universidad de Los Andes, Bogota, Colombia*
[18]*University of Split, Faculty of Electrical Engineering, Mechanical Engineering and Naval Architecture, Split, Croatia*
[19]*University of Split, Faculty of Science, Split, Croatia*
[20]*Institute Rudjer Boskovic, Zagreb, Croatia*
[21]*University of Cyprus, Nicosia, Cyprus*
[22]*Charles University, Prague, Czech Republic*
[23]*Academy of Scientific Research and Technology of the Arab Republic of Egypt, Egyptian Network of High Energy Physics, Cairo, Egypt*
[24]*National Institute of Chemical Physics and Biophysics, Tallinn, Estonia*
[25]*Department of Physics, University of Helsinki, Helsinki, Finland*
[26]*Helsinki Institute of Physics, Helsinki, Finland*
[27]*Lappeenranta University of Technology, Lappeenranta, Finland*
[28]*DSM/IRFU, CEA/Saclay, Gif-sur-Yvette, France*
[29]*Laboratoire Leprince-Ringuet, Ecole Polytechnique, IN2P3-CNRS, Palaiseau, France*

[30]*Institut Pluridisciplinaire Hubert Curien, Université de Strasbourg, Université de Haute Alsace Mulhouse, CNRS/IN2P3, Strasbourg, France*
[31]*Centre de Calcul de l'Institut National de Physique Nucleaire et de Physique des Particules, CNRS/IN2P3, Villeurbanne, France*
[32]*Université de Lyon, Université Claude Bernard Lyon 1, CNRS-IN2P3, Institut de Physique Nucléaire de Lyon, Villeurbanne, France*
[33]*Georgian Technical University, Tbilisi, Georgia*
[34]*Tbilisi State University, Tbilisi, Georgia*
[35]*RWTH Aachen University, I. Physikalisches Institut, Aachen, Germany*
[36]*RWTH Aachen University, III. Physikalisches Institut A, Aachen, Germany*
[37]*RWTH Aachen University, III. Physikalisches Institut B, Aachen, Germany*
[38]*Deutsches Elektronen-Synchrotron, Hamburg, Germany*
[39]*University of Hamburg, Hamburg, Germany*
[40]*Institut für Experimentelle Kernphysik, Karlsruhe, Germany*
[41]*Institute of Nuclear and Particle Physics (INPP), NCSR Demokritos, Aghia Paraskevi, Greece*
[42]*University of Athens, Athens, Greece*
[43]*University of Ioánnina, Ioánnina, Greece*
[44]*Wigner Research Centre for Physics, Budapest, Hungary*
[45]*Institute of Nuclear Research ATOMKI, Debrecen, Hungary*
[46]*University of Debrecen, Debrecen, Hungary*
[47]*National Institute of Science Education and Research, Bhubaneswar, India*
[48]*Panjab University, Chandigarh, India*
[49]*University of Delhi, Delhi, India*
[50]*Saha Institute of Nuclear Physics, Kolkata, India*
[51]*Bhabha Atomic Research Centre, Mumbai, India*
[52]*Tata Institute of Fundamental Research, Mumbai, India*
[53]*Indian Institute of Science Education and Research (IISER), Pune, India*
[54]*Institute for Research in Fundamental Sciences (IPM), Tehran, Iran*
[55]*University College Dublin, Dublin, Ireland*
[56a]*INFN Sezione di Bari, Bari, Italy*
[56b]*Università di Bari, Bari, Italy*
[56c]*Politecnico di Bari, Bari, Italy*
[57a]*INFN Sezione di Bologna, Bologna, Italy*
[57b]*Università di Bologna, Bologna, Italy*
[58a]*INFN Sezione di Catania, Catania, Italy*
[58b]*Università di Catania, Catania, Italy*
[58c]*CSFNSM, Catania, Italy*
[59a]*INFN Sezione di Firenze, Firenze, Italy*
[59b]*Università di Firenze, Firenze, Italy*
[60]*INFN Laboratori Nazionali di Frascati, Frascati, Italy*
[61a]*INFN Sezione di Genova, Genova, Italy*
[61b]*Università di Genova, Genova, Italy*
[62a]*INFN Sezione di Milano-Bicocca, Milano, Italy*
[62b]*Università di Milano-Bicocca, Milano, Italy*
[63a]*INFN Sezione di Napoli, Napoli, Italy*
[63b]*Università di Napoli 'Federico II', Napoli, Italy*
[63c]*Università della Basilicata, Roma, Italy*
[63d]*Università G. Marconi, Roma, Italy*
[64a]*INFN Sezione di Padova, Padova, Italy*
[64b]*Università di Padova, Padova, Italy*
[64c]*Università di Trento, Trento, Italy*
[65a]*INFN Sezione di Pavia, Pavia, Italy*
[65b]*Università di Pavia, Pavia, Italy*
[66a]*INFN Sezione di Perugia, Perugia, Italy*
[66b]*Università di Perugia, Perugia, Italy*
[67a]*INFN Sezione di Pisa, Pisa, Italy*
[67b]*Università di Pisa, Pisa, Italy*
[67c]*Scuola Normale Superiore di Pisa, Pisa, Italy*
[68a]*INFN Sezione di Roma, Roma, Italy*
[68b]*Università di Roma, Roma, Italy*

[69a]INFN Sezione di Torino, Torino, Italy
[69b]Università di Torino, Torino, Italy
[69c]Università del Piemonte Orientale, Novara, Italy
[70a]INFN Sezione di Trieste, Trieste, Italy
[70b]Università di Trieste, Trieste, Italy
[71]Kangwon National University, Chunchon, Korea
[72]Kyungpook National University, Daegu, Korea
[73]Chonbuk National University, Jeonju, Korea
[74]Chonnam National University, Institute for Universe and Elementary Particles, Kwangju, Korea
[75]Korea University, Seoul, Korea
[76]Seoul National University, Seoul, Korea
[77]University of Seoul, Seoul, Korea
[78]Sungkyunkwan University, Suwon, Korea
[79]Vilnius University, Vilnius, Lithuania
[80]National Centre for Particle Physics, Universiti Malaya, Kuala Lumpur, Malaysia
[81]Centro de Investigacion y de Estudios Avanzados del IPN, Mexico City, Mexico
[82]Universidad Iberoamericana, Mexico City, Mexico
[83]Benemerita Universidad Autonoma de Puebla, Puebla, Mexico
[84]Universidad Autónoma de San Luis Potosí, San Luis Potosí, Mexico
[85]University of Auckland, Auckland, New Zealand
[86]University of Canterbury, Christchurch, New Zealand
[87]National Centre for Physics, Quaid-I-Azam University, Islamabad, Pakistan
[88]National Centre for Nuclear Research, Swierk, Poland
[89]Institute of Experimental Physics, Faculty of Physics, University of Warsaw, Warsaw, Poland
[90]Laboratório de Instrumentação e Física Experimental de Partículas, Lisboa, Portugal
[91]Joint Institute for Nuclear Research, Dubna, Russia
[92]Petersburg Nuclear Physics Institute, Gatchina (St. Petersburg), Russia
[93]Institute for Nuclear Research, Moscow, Russia
[94]Institute for Theoretical and Experimental Physics, Moscow, Russia
[95]National Research Nuclear University 'Moscow Engineering Physics Institute' (MEPhI), Moscow, Russia
[96]P.N. Lebedev Physical Institute, Moscow, Russia
[97]Skobeltsyn Institute of Nuclear Physics, Lomonosov Moscow State University, Moscow, Russia
[98]State Research Center of Russian Federation, Institute for High Energy Physics, Protvino, Russia
[99]University of Belgrade, Faculty of Physics and Vinca Institute of Nuclear Sciences, Belgrade, Serbia
[100]Centro de Investigaciones Energéticas Medioambientales y Tecnológicas (CIEMAT), Madrid, Spain
[101]Universidad Autónoma de Madrid, Madrid, Spain
[102]Universidad de Oviedo, Oviedo, Spain
[103]Instituto de Física de Cantabria (IFCA), CSIC-Universidad de Cantabria, Santander, Spain
[104]CERN, European Organization for Nuclear Research, Geneva, Switzerland
[105]Paul Scherrer Institut, Villigen, Switzerland
[106]Institute for Particle Physics, ETH Zurich, Zurich, Switzerland
[107]Universität Zürich, Zurich, Switzerland
[108]National Central University, Chung-Li, Taiwan
[109]National Taiwan University (NTU), Taipei, Taiwan
[110]Chulalongkorn University, Faculty of Science, Department of Physics, Bangkok, Thailand
[111]Cukurova University, Adana, Turkey
[112]Middle East Technical University, Physics Department, Ankara, Turkey
[113]Bogazici University, Istanbul, Turkey
[114]Istanbul Technical University, Istanbul, Turkey
[115]Institute for Scintillation Materials of National Academy of Science of Ukraine, Kharkov, Ukraine
[116]National Scientific Center, Kharkov Institute of Physics and Technology, Kharkov, Ukraine
[117]University of Bristol, Bristol, United Kingdom
[118]Rutherford Appleton Laboratory, Didcot, United Kingdom
[119]Imperial College, London, United Kingdom
[120]Brunel University, Uxbridge, United Kingdom
[121]Baylor University, Waco 76798, USA
[122]The University of Alabama, Tuscaloosa 35487, USA
[123]Boston University, Boston 02215, USA
[124]Brown University, Providence 02912, USA

[125]University of California, Davis 95616, USA
[126]University of California, Los Angeles 90095, USA
[127]University of California, Riverside 92521, USA
[128]University of California, San Diego, La Jolla 92093, USA
[129]University of California, Santa Barbara 93106, USA
[130]California Institute of Technology, Pasadena 91125, USA
[131]Carnegie Mellon University, Pittsburgh 15213, USA
[132]University of Colorado Boulder, Boulder 80309, USA
[133]Cornell University, Ithaca 14853, USA
[134]Fermi National Accelerator Laboratory, Batavia 60510, USA
[135]University of Florida, Gainesville 32611, USA
[136]Florida International University, Miami 33199, USA
[137]Florida State University, Tallahassee 32306, USA
[138]Florida Institute of Technology, Melbourne 32901, USA
[139]University of Illinois at Chicago (UIC), Chicago 60607, USA
[140]The University of Iowa, Iowa City 52242, USA
[141]Johns Hopkins University, Baltimore 21218, USA
[142]The University of Kansas, Lawrence 66045, USA
[143]Kansas State University, Manhattan 66506, USA
[144]Lawrence Livermore National Laboratory, Livermore 94551, USA
[145]University of Maryland, College Park 20742, USA
[146]Massachusetts Institute of Technology, Cambridge 02139, USA
[147]University of Minnesota, Minneapolis 55455, USA
[148]University of Mississippi, Oxford 38677, USA
[149]University of Nebraska-Lincoln, Lincoln 68588, USA
[150]State University of New York at Buffalo, Buffalo 14260, USA
[151]Northeastern University, Boston 02115, USA
[152]Northwestern University, Evanston 60208, USA
[153]University of Notre Dame, Notre Dame 46556, USA
[154]The Ohio State University, Columbus 43210, USA
[155]Princeton University, Princeton 08542, USA
[156]University of Puerto Rico, Mayaguez 00681, USA
[157]Purdue University, West Lafayette 47907, USA
[158]Purdue University Calumet, Hammond 46323, USA
[159]Rice University, Houston 77251, USA
[160]University of Rochester, Rochester 14627, USA
[161]The Rockefeller University, New York 10021, USA
[162]Rutgers, The State University of New Jersey, Piscataway 08854, USA
[163]University of Tennessee, Knoxville 37996, USA
[164]Texas A&M University, College Station 77843, USA
[165]Texas Tech University, Lubbock 79409, USA
[166]Vanderbilt University, Nashville 37235, USA
[167]University of Virginia, Charlottesville 22904, USA
[168]Wayne State University, Detroit 48202, USA
[169]University of Wisconsin, Madison 53706, USA

[a]Deceased.
[b]Also at Vienna University of Technology, Vienna, Austria.
[c]Also at CERN, European Organization for Nuclear Research, Geneva, Switzerland.
[d]Also at State Key Laboratory of Nuclear Physics and Technology, Peking University, Beijing, China.
[e]Also at Institut Pluridisciplinaire Hubert Curien, Université de Strasbourg, Université de Haute Alsace Mulhouse, CNRS/IN2P3, Strasbourg, France.
[f]Also at National Institute of Chemical Physics and Biophysics, Tallinn, Estonia.
[g]Also at Skobeltsyn Institute of Nuclear Physics, Lomonosov Moscow State University, Moscow, Russia.
[h]Also at Universidade Estadual de Campinas, Campinas, Brazil.
[i]Also at Centre National de la Recherche Scientifique (CNRS)—IN2P3, Paris, France.
[j]Also at Laboratoire Leprince-Ringuet, Ecole Polytechnique, IN2P3-CNRS, Palaiseau, France.
[k]Also at Joint Institute for Nuclear Research, Dubna, Russia.
[l]Also at Beni-Suef University, Bani Sweif, Egypt.
[m]Also at British University in Egypt, Cairo, Egypt.

[n]Also at Ain Shams University, Cairo, Egypt.
[o]Also at Zewail City of Science and Technology, Zewail, Egypt.
[p]Also at Université de Haute Alsace, Mulhouse, France.
[q]Also at Tbilisi State University, Tbilisi, Georgia.
[r]Also at University of Hamburg, Hamburg, Germany.
[s]Also at Brandenburg University of Technology, Cottbus, Germany.
[t]Also at Institute of Nuclear Research ATOMKI, Debrecen, Hungary.
[u]Also at Eötvös Loránd University, Budapest, Hungary.
[v]Also at University of Debrecen, Debrecen, Hungary.
[w]Also at Wigner Research Centre for Physics, Budapest, Hungary.
[x]Also at University of Visva-Bharati, Santiniketan, India.
[y]Also at King Abdulaziz University, Jeddah, Saudi Arabia.
[z]Also at University of Ruhuna, Matara, Sri Lanka.
[aa]Also at Isfahan University of Technology, Isfahan, Iran.
[bb]Also at University of Tehran, Department of Engineering Science, Tehran, Iran.
[cc]Also at Plasma Physics Research Center, Science and Research Branch, Islamic Azad University, Tehran, Iran.
[dd]Also at Università degli Studi di Siena, Siena, Italy.
[ee]Also at Purdue University, West Lafayette, USA.
[ff]Also at International Islamic University of Malaysia, Kuala Lumpur, Malaysia.
[gg]Also at Malaysian Nuclear Agency, MOSTI, Kajang, Malaysia.
[hh]Also at Consejo Nacional de Ciencia y Tecnología, Mexico city, Mexico.
[ii]Also at Warsaw University of Technology, Institute of Electronic Systems, Warsaw, Poland.
[jj]Also at Institute for Nuclear Research, Moscow, Russia.
[kk]Also at St. Petersburg State Polytechnical University, St. Petersburg, Russia.
[ll]Also at National Research Nuclear University 'Moscow Engineering Physics Institute' (MEPhI), Moscow, Russia.
[mm]Also at California Institute of Technology, Pasadena, USA.
[nn]Also at Faculty of Physics, University of Belgrade, Belgrade, Serbia.
[oo]Also at Facoltà Ingegneria, Università di Roma, Roma, Italy.
[pp]Also at National Technical University of Athens, Athens, Greece.
[qq]Also at Scuola Normale e Sezione dell'INFN, Pisa, Italy.
[rr]Also at University of Athens, Athens, Greece.
[ss]Also at Institute for Theoretical and Experimental Physics, Moscow, Russia.
[tt]Also at Albert Einstein Center for Fundamental Physics, Bern, Switzerland.
[uu]Also at Gaziosmanpasa University, Tokat, Turkey.
[vv]Also at Mersin University, Mersin, Turkey.
[ww]Also at Cag University, Mersin, Turkey.
[xx]Also at Piri Reis University, Istanbul, Turkey.
[yy]Also at Adiyaman University, Adiyaman, Turkey.
[zz]Also at Ozyegin University, Istanbul, Turkey.
[aaa]Also at Izmir Institute of Technology, Izmir, Turkey.
[bbb]Also at Mimar Sinan University, Istanbul, Istanbul, Turkey.
[ccc]Also at Marmara University, Istanbul, Turkey.
[ddd]Also at Kafkas University, Kars, Turkey.
[eee]Also at Yildiz Technical University, Istanbul, Turkey.
[fff]Also at Hacettepe University, Ankara, Turkey.
[ggg]Also at Rutherford Appleton Laboratory, Didcot, United Kingdom.
[hhh]Also at School of Physics and Astronomy, University of Southampton, Southampton, United Kingdom.
[iii]Also at Instituto de Astrofísica de Canarias, La Laguna, Spain.
[jjj]Also at Utah Valley University, Orem, USA.
[kkk]Also at University of Belgrade, Faculty of Physics and Vinca Institute of Nuclear Sciences, Belgrade, Serbia.
[lll]Also at Argonne National Laboratory, Argonne, USA.
[mmm]Also at Erzincan University, Erzincan, Turkey.
[nnn]Also at Texas A&M University at Qatar, Doha, Qatar.
[ooo]Also at Kyungpook National University, Daegu, Korea.